ELECTROWEAK PHYSICS RESULTS FROM THE DØ EXPERIMENT AT FERMILAB[1]

JOHN ELLISON

Physics Department, University of California,

Riverside, CA 92521, USA

for the DØ Collaboration

ABSTRACT

We present electroweak physics results from the DØ experiment using data from $p\bar{p}$ collisions at $\sqrt{s}$ = 1.8 TeV, concentrating on *single* W and Z production cross sections and the production of electroweak gauge boson *pairs*. The inclusive cross sections times branching ratios for W and Z production have been measured and are used to determine the inclusive width of the W boson. Direct tests of the $WW\gamma$ and WWZ trilinear gauge boson couplings are derived from the study of diboson production. These measurements test the non-abelian self couplings of the W, Z and photon, one of the most direct consequences of the $SU(2)_L \times U(1)_Y$ gauge symmetry. We present measurements of the $WW\gamma$ coupling based on $p\bar{p} \rightarrow l\nu\gamma + X$ $(l = e, \mu)$ and limits on anomalous WWZ and $WW\gamma$ couplings based on searches for $p\bar{p} \rightarrow W^+W^- + X \rightarrow ll'\nu\bar{\nu} + X$ and $p\bar{p} \rightarrow WW / WZ + X \rightarrow e\nu + \text{jets} + X$. We also present limits on the $ZZ\gamma$ and $Z\gamma\gamma$ couplings based on $p\bar{p} \rightarrow l\bar{l}\gamma + X$ events.

1. Introduction

The DØ detector at the Fermilab Tevatron $p\bar{p}$ collider collected data corresponding to an integrated luminosity of 15 pb^{-1} in its first data taking run ("Run 1a") from 1992–93 and 88 pb^{-1} in its second run ("Run 1b") during 1994–95. In this paper we present some results on electroweak physics from the analysis of a subset of this data (mainly that from Run 1a).

The experimental study of the physics of electroweak gauge bosons began in 1983 with the discovery of the W and Z bosons at the CERN $S p\bar{p} S$ [1]. The production of W and Z bosons in much larger numbers has subsequently been possible at LEP, SLC and the Tevatron. The Tevatron data allows refined measurements of the W boson properties, such as its mass and width, with improved precision, and *new* studies of the physics of electroweak boson pair production. In this paper we concentrate on the latter topic (sections

---

3–6). As a prelude we present the measurements of the W and Z production cross sections (section 2).

2. W and Z Production and the Inclusive Width of the W Boson

The measurement of the production cross-sections times branching ratios ($\sigma \cdot B$) for the W and Z bosons allows a determination of the width of the W boson and a comparison of W and Z boson production with QCD predictions.

The first DØ measurement of $\sigma \cdot B$ was performed using data collected in Run 1a corresponding to a total integrated luminosity of approximately 12 pb^{-1} for the triggers used for W and Z event filtering.

Measurement of the cross sections were made using the e,μ decay mode channels. Measurements using τ decays and qq decays are experimentally challenging due to the low efficiency of τ detection and very high QCD background in the dijet channel. The decay channels used in this analysis are $W \to e\nu$, $W \to \mu\nu$, $Z \to e^+e^-$ and $Z \to \mu^+\mu^-$. Events were selected from single lepton triggers and offline were required to contain a high p_T isolated lepton plus missing transverse energy (W events) or two high p_T isolated leptons (Z events), one passing the standard identification cuts and the second passing less stringent "loose" cuts. The selection criteria are summarized in Table 1. Details of the DØ detector and particle identification criteria are given in [2,3].

	$W \to e\nu$	$Z \to e^-e^-$	$W \to \mu\nu$	$Z \to \mu^+\mu^-$
Selection Cuts:				
E_T^{l1} (GeV)	25	25	20	20
E_T^{l2} or $\not{E}_T$ (GeV)	25	25	20	15
Lepton η	$|\eta|<1.1$ or $1.5<|\eta|<2.5$		$|\eta|<1.0$	
No. Candidates	10338	775	1665	77
Backgrounds (%):				
$Z \to ll$	0.6 ± 0.1	–	7.3 ± 0.5	0.7 ± 0.2
$W \to \tau\nu$	1.8 ± 0.1	–	5.9 ± 0.5	–
QCD	3.3 ± 0.5	2.8 ± 1.4	5.1 ± 0.8	2.6 ± 0.8
Cosmic	–	–	3.8 ± 1.6	5.1 ± 3.6
Drell-Yan	–	1.2 ± 0.1	–	1.7 ± 0.3
Total	5.7 ± 0.5	4.0 ± 1.4	22.1 ± 1.9	10.1 ± 3.7
Acceptance (%)	46.0 ± 0.6	36.3 ± 0.4	24.8 ± 0.7	6.5 ± 0.4
Efficiency (%)	70.4 ± 1.7	73.6 ± 2.4	21.9 ± 2.6	52.7 ± 4.9
$\int Ldt$ (pb^{-1})	12.8 ± 0.7	12.8 ± 0.7	11.4 ± 0.6	11.4 ± 0.6
$\sigma \cdot B$ (nb)	2.36	0.218	2.09	0.178
stat error	±0.02	±0.008	±0.06	±0.022
syst error	±0.07	±0.008	±0.22	±0.021
lum error	±0.13	±0.012	±0.11	±0.009

Table 1. Summary of analysis and production cross section times branching ratio results for W and Z bosons.

Figure 1 shows the transverse mass spectra for $W \to e\nu$ and $W \to \mu\nu$ events and the invariant mass spectra for $Z \to e^+e^-$ and $Z \to \mu^+\mu^-$ events (data points) together with the background estimates (shaded histograms) and the sum of the background distributions and a Monte Carlo simulation of the signal, using GEANT [4] to model the DØ detector. The backgrounds, ranging between 4% to 22% of the signal, depending on the channel, are listed in Table 1.

The values of $\sigma \cdot B$ were calculated by subtracting the background from the number of observed events and dividing by the acceptance, efficiency and integrated luminosity. The results are shown in Table 1 and are plotted in Fig. 2, together with the CDF results from the same collider run and *preliminary* DØ results using ≈ 30 pb^{-1} of data from the most recent data taking run (Run 1b). The measurements agree well with the order α_s^2 QCD predictions of $\sigma_W \cdot B(W \to l\nu) = 2.42^{+0.13}_{-0.11}$ nb and $\sigma_Z \cdot B(Z \to ll) = 0.226^{+0.011}_{-0.009}$ nb, shown as the shaded bands in Fig. 2. The CTEQ2M parton distribution functions [5] were used to calculate the central values.

The inclusive width of the W boson is calculated using the measured ratio (R) of the W and Z $\sigma \cdot B$ values:

$$R = \frac{\sigma_W \cdot B(W \to l\nu)}{\sigma_Z \cdot B(Z \to ll)} \quad \text{with} \quad B(W \to l\nu) = \frac{\Gamma(W \to l\nu)}{\Gamma(W)}.$$

Combining the DØ Run 1a electron and muon channel data yields $R_{e+\mu} = 10.89 \pm 0.49\,(\text{stat} \oplus \text{syst})$. Many common sources of error cancel in R, including the uncertainty in the integrated luminosity and parts of the errors in the acceptance and event selection efficiency. The theoretical calculation $\sigma_W/\sigma_Z = 3.33 \pm 0.03$ [3,6] and the LEP measurement $B(Z \to ll) = (3.367 \pm 0.006)\%$ [7] are then used to obtain $B(W \to l\nu) = (11.02 \pm 0.50)\%$. We combine this measurement of $B(W \to l\nu)$ with a theoretical calculation [3,8] of $\Gamma(W \to l\nu) = 225.2 \pm 1.5$ MeV to obtain an indirect measurement of the W inclusive width:

$$\Gamma(W) = 2.044 \pm 0.093 \text{ GeV}.$$

Figure 3 summarizes the measurements of $\Gamma(W)$ to date. The world average of 2.062 ± 0.059 GeV can be compared with the Standard Model (SM) prediction of 2.077 ± 0.014 GeV [3,8] to set limits on non-standard decays of the W. At the 95% confidence level, the upper limit on the width due to non-standard decays (*e.g.* decays to heavy quarks or to SUSY particles such as charginos and neutralinos) is 109 MeV.
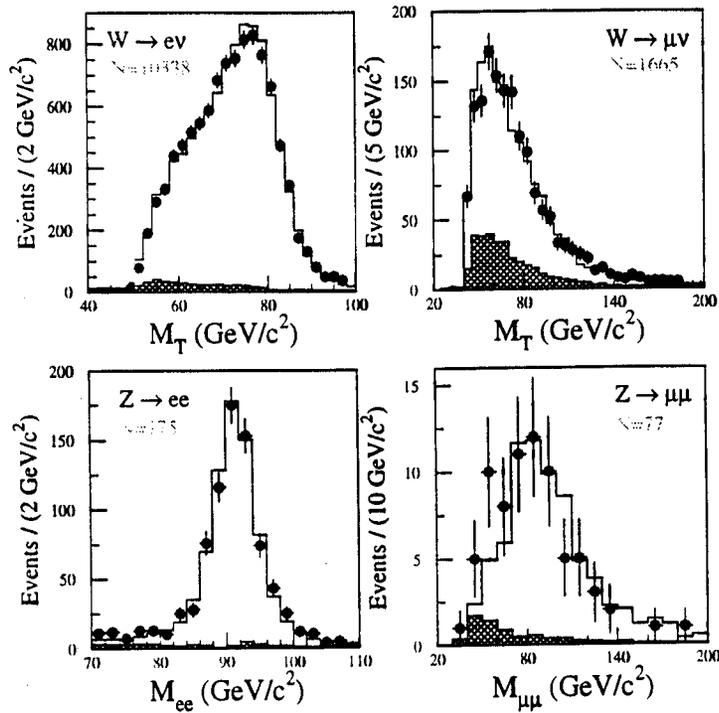
Fig. 1. Transverse mass and invariant mass distributions for the W and Z candidate events (points). The shaded histograms show the total estimated backgrounds and the open histogram is the sum of the SM signal plus the total background.
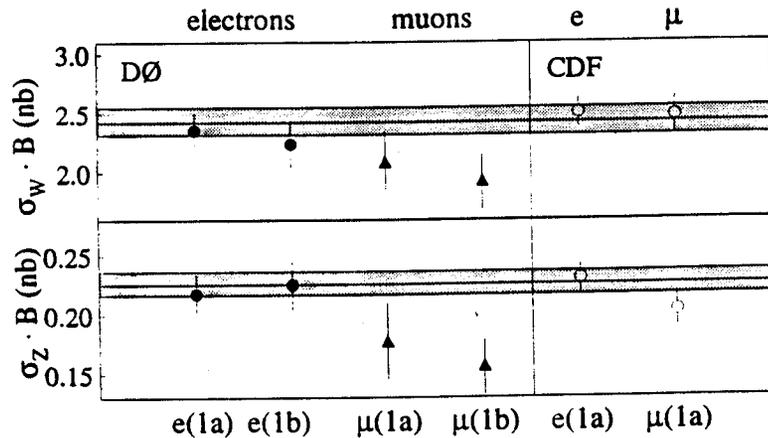

Fig. 2. Measurements of the W and Z inclusive cross-sections times branching ratios from DØ (solid points). Also shown are the measurements from CDF (open points) and the SM theoretical predictions (shaded bands show central values and $\pm 1\sigma$ uncertainties). The central values were obtained using the CTEQ2M parton distribution functions [5].

4
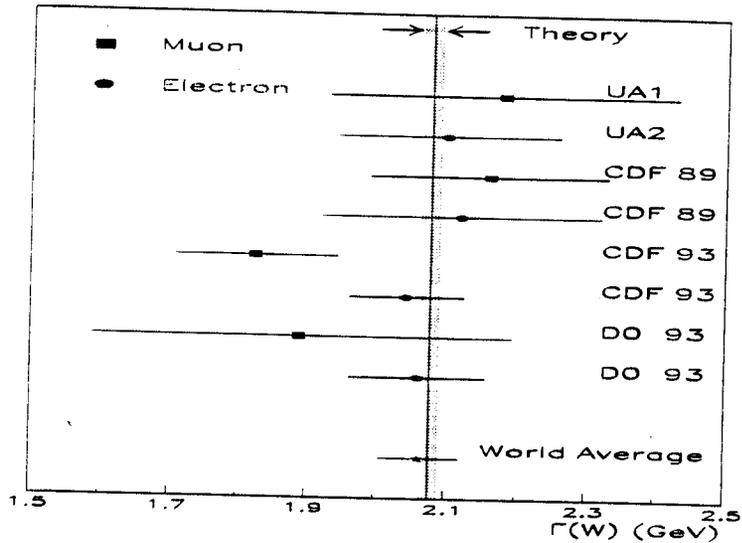
Fig. 3. Measurements of the W width from the Tevatron and CERN compared with the SM theoretical prediction (band shows $\pm 1\sigma$ uncertainties).

3. Diboson Production and the Gauge Boson Couplings

The production of electroweak boson pairs at hadron colliders is particularly interesting since these processes probe the nature of the non-Abelian gauge boson self-couplings of the Standard Model (*i.e.* the $WW\gamma$, WWZ couplings). These processes are also sensitive to deviations from the tree level SM couplings, which may arise due to compositeness of the W and Z bosons or loop corrections to the vertex factors as shown in the examples of Fig. 4. These effects may also result in non-zero $ZZ\gamma$ and $Z\gamma\gamma$ couplings which can be tested via $Z\gamma$ production. In the SM these couplings are zero since the Z is a neutral particle and does not couple to the neutral photon[2].

To test the agreement with the SM and to evaluate the sensitivity to anomalous couplings we use a phenomenological effective Lagrangian for the WWV ($V=\gamma,Z$) vertex, assuming electromagnetic gauge invariance, and invariance under Lorentz and CP transformations[3] [9]:

$$i\mathcal{L}_{eff}^{WWV} = g_{WWV}\left[g_1^V (W_{\mu\nu}^\dagger W^\mu - W^{\dagger\mu}W_{\mu\nu})V^\nu + \kappa_V W_\mu^\dagger W_\nu V^{\mu\nu} + \frac{\lambda_V}{m_W^2} W_{\rho\mu}^\dagger W_\nu^\mu V^{\nu\rho} \right]$$

where W^μ and V^μ are the W and V fields respectively, $g_{WW\gamma} = -e$, $g_{WWZ} = -e\cot\theta_W$ and g_1^V, κ_V, and λ_V are dimensionless coupling parameters. In the SM at tree level $g_1^V = 1$, $\kappa_V = 1$, and $\lambda_V = 0$. Assuming that the coupling parameters for the $WW\gamma$ and WWZ vertices are equal, only two parameters remain:

---

[2] Both the photon and Z have zero electric charge and zero weak isospin.
[3] CP violating operators may also be introduced in the Lagrangian, but for simplicity, we do not consider them here.

$$\kappa_\gamma = \kappa_Z = \kappa \quad (\text{or } \Delta\kappa \equiv \kappa - 1)$$
$$\lambda_\gamma = \lambda_Z = \lambda.$$

The coupling parameters are related to the lowest order terms in a multipole expansion of photon interactions with the W boson, $e.g.$ the W magnetic dipole moment is given by $\mu_W = (e/2m_W)\left(g_1^\gamma + \kappa_\gamma + \lambda_\gamma\right)$.

A similar formalism is used to describe the $Z\gamma V$ $(V=\gamma,Z)$ vertices. It is conventional to parametrize the couplings in terms of the $Z\gamma V$ vertex functions [9]:

$$\Gamma_{Z\gamma V}^{\alpha\beta\mu}(q_1,q_2,P) = \frac{P^2 - m_V^2}{m_Z^2}\left[h_3^V \varepsilon^{\mu\alpha\beta\rho} q_{2\rho} + \frac{h_4^V}{m_Z^2} P^\alpha \varepsilon^{\mu\beta\rho\sigma} P_\rho q_{2\sigma} \right]$$

where h_3^V, h_4^V are dimensionless coupling parameters, q_1, q_2 and P are the 4-momenta of the Z, γ and V respectively. In the SM at tree level (no coupling of the γ to the Z) $h_3^V = 0, h_4^V = 0$.

All interaction Lagrangians with constant anomalous couplings violate unitarity at high energy and so the coupling parameters must be modified to include form factors, e.g.

$$\Delta\kappa(q^2) = \frac{\Delta\kappa^0}{(1 + q^2/\Lambda^2)^n}$$

where $\Delta\kappa^0$ = value of coupling parameter at $q^2 = 0$[4], $q^2 = \hat{s}$ = square of the invariant mass of the $W\gamma$ system, $n = 2$ for a dipole form factor and Λ = form factor scale (a function of the scale of new physics). We take $n=2$ for $\Delta\kappa$ and λ. For h_3^V we take $n=3$ and for h_4^V $n=4$, which ensures that unitarity is satisfied and that both terms have the same high energy behavior [10]. Note that in the SM delicate cancellations (such as those between the first three Feynman graphs in Fig. 5) ensure that unitarity is satisfied. Constant anomalous couplings would destroy these cancellations leading to violation of unitarity.
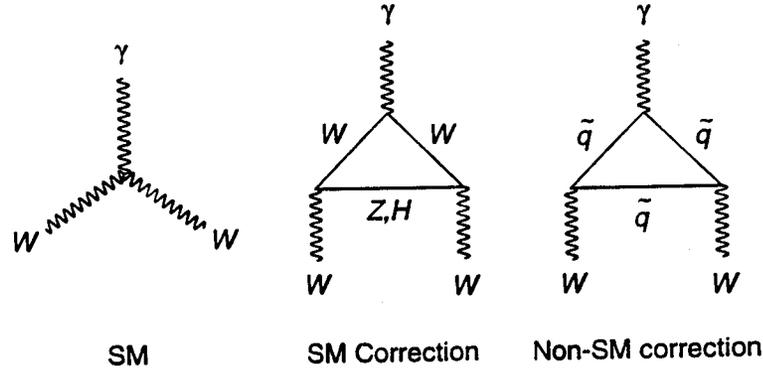

Fig. 4.   Standard Model $WW\gamma$ vertex (left) and examples of loop corrections leading to deviations from the tree-level SM vertex functions.

---

[4] The notations for the other couplings defined at $q^2 = 0$ are λ^0, h_{30}^V and h_{40}^V.

4. $W\gamma$ Production and the $WW\gamma$ Coupling

$W\gamma$ production at the Tevatron can be used to probe the $WW\gamma$ coupling [11]. The Feynman diagrams for the processes contributing to $p\bar{p} \rightarrow l\nu\gamma + X$ are shown in Fig. 5. The u- and t-channel diagrams correspond to photon bremsstrahlung from an initial state quark, whereas the s-channel diagram is sensitive to the $WW\gamma$ vertex. Events in which a photon is radiated from the final state lepton from single W decay also result in the same $l\nu\gamma$ final state. These radiative decay events can be suppressed by imposing a cut on the photon-lepton angular separation and further by requiring the lepton-photon-neutrino transverse cluster mass[5] $M_T(l\gamma;\nu)$ to be $> M_W$. Non-SM values of the $WW\gamma$ coupling (Fig. 5 (c)) result in an increase in the total cross-section and an enhacement of events with high-E_T photons. This is the experimental signature which we use to test for anomalous couplings.
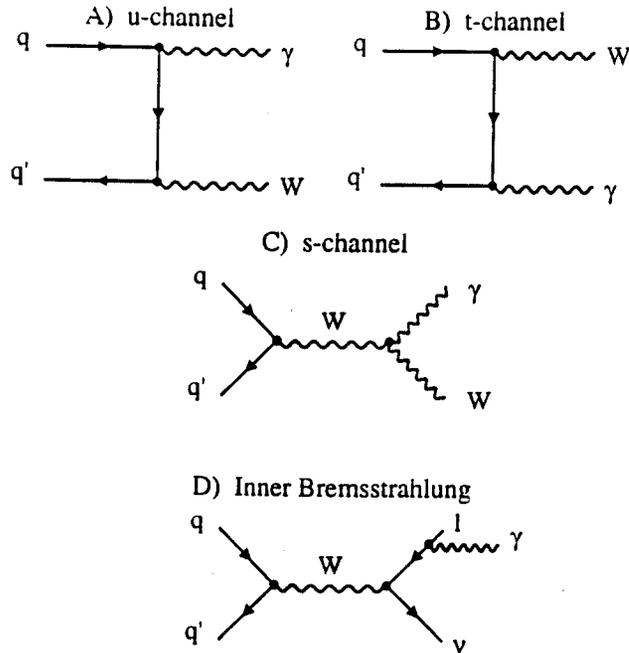
Fig. 5.   Feynman diagrams contributing to the process $p\bar{p} \rightarrow l\nu\gamma$.

We selected a sample of $W(e\nu)\gamma$ candidates from events passing a trigger which requires an isolated EM cluster with $E_T > 20$ GeV and missing transverse energy

---

[5] The transverse cluster mass is defined by $M_T^2(l\gamma;\nu) = \left[\left(m_{\gamma l}^2 + \left|E_T^\gamma + E_T^l\right|^2\right)^{1/2} + \not{E}_T\right]^2 - \left|E_T^\gamma + E_T^l + \not{E}_T\right|^2$ where $m_{\gamma l}$ is the photon–lepton invariant mass, E_T^γ and E_T^l are the photon and lepton transverse energy vectors respectively and $\not{E}_T$ is the missing transverse energy vector.

$(\not{E}_T) > 20$ GeV. This EM cluster was required to be within the fiducial region of the calorimeter, $|\eta| < 1.1$, and at least 0.01 radians away from the azimuthal boundaries between the 32 EM modules in the central calorimeter, or within $1.5 < |\eta| < 2.5$ in the end calorimeters. The offline kinematic selection was made requiring $E_T^e > 25$ GeV, $\not{E}_T > 25$ GeV and a transverse mass $M_T > 40$ GeV. The electron was required to satisfy electron identification criteria as described in [12].

The $W(\mu\nu)\gamma$ sample was selected from a trigger requiring an EM cluster with $E_T > 7$ GeV and a muon track with $p_T > 5$ GeV in the region $|\eta| < 1.7$. Kinematic selection was made requiring $p_T^\mu > 15$ GeV and $\not{E}_T > 15$ GeV. Muon tracks were required to satisfy standard muon identification requirements [12]. To reduce the background due to $Z(\mu\mu)\gamma$ production, events were rejected if they contained an extra muon track with $p_T > 8$ GeV.

The requirements on photons were common to both the electron and muon channel samples. We required $E_T^\gamma > 10$ GeV and the same geometrical and quality selection as for electrons, except that we required a tighter isolation, $I < 0.10$, and that there be no track matching the calorimeter cluster. The isolation parameter is defined as $I = [E(0.4) - EM(0.2)]/EM(0.2)$, where E(0.4) is total calorimeter energy inside a cone of radius $R=0.4$ and EM(0.2) is the electromagnetic energy in a cone of radius $R=0.2$. In addition, we required that the separation between the photon and lepton be $\Delta R_{l\gamma} > 0.7$. This requirement suppresses the radiative W decay events as described above, and minimizes the probability for a photon cluster to merge with a nearby calorimeter cluster associated with an electron or a muon. The above selection criteria yielded 11 $W(e\nu)\gamma$ candidates and 12 $W(\mu\nu)\gamma$ candidates.

The backgrounds are from $W + $jet(s) production, where a jet is misidentified as a photon; $Z(ll)\gamma$ production where one of the leptons from the Z is undetected or mismeasured by the detector; and $W\gamma$ with $W \rightarrow \tau\nu$ followed by $\tau \rightarrow l\nu\bar{\nu}$. The first was determined from DØ data using the probability that a jet fakes a photon $P(j \rightarrow \gamma)$ which was estimated using multijet events (Fig. 6). The $Z\gamma$ background was estimated using the $Z\gamma$ event generator of Baur and Berger [10] and the background from τ decays was obtained using the ISAJET program [13]. The $W + $jet(s) process was the dominant source of background in the electron channel while in the muon channel the $Z\gamma$ background was larger. This is due to the geometrical acceptance of the muon detector system and muon chamber inefficiencies.

	$W(e\nu)\gamma$	$W(\mu\nu)\gamma$
Selection Cuts:		
p_T^l	25	15
$\not{E}_T$	25	15
E_T^γ	10	10
Lepton η	$|\eta|<1.1$ or $1.5<|\eta|<2.5$	$|\eta|<1.7$
Photon η	$|\eta|<1.1$ or $1.5<|\eta|<2.5$	
No. Candidates	11	12
Backgrounds:		
$W+$jet(s)	1.7 ± 0.9	1.3 ± 0.7
$Z\gamma$	0.11 ± 0.02	2.7 ± 0.8
$W(\tau\nu)\gamma$	0.17 ± 0.02	0.4 ± 0.1
Total	2.0 ± 0.9	4.4 ± 1.1

Table 2.   Summary of $W(e\nu)\gamma$ and $W(\mu\nu)\gamma$ selection, data and backgrounds.
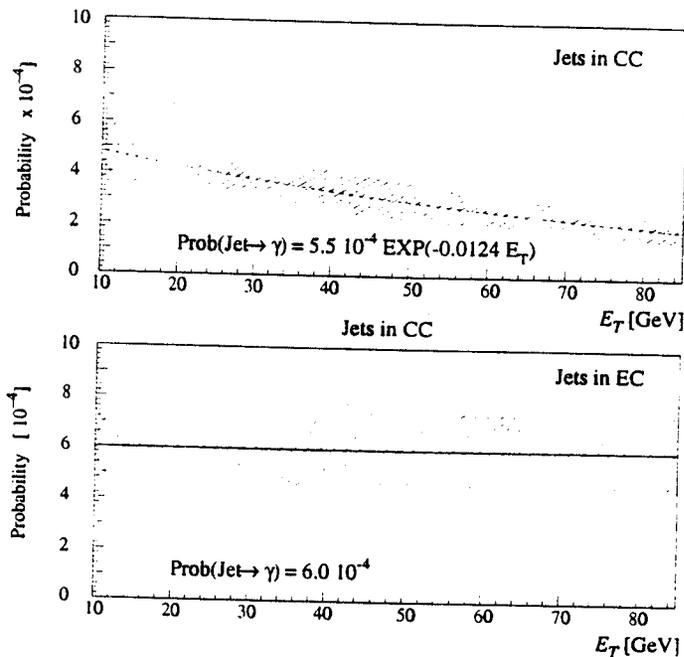
Fig. 6.   Probability that a jet fakes a photon as a function of E_T in the central calorimeter (top) and end calorimeters (bottom). The shadded band shows the estimated error.

The SM prediction for the number of events observed was obtained using the $W\gamma$ event generator of Baur and Zeppenfeld [14] together with a Monte Carlo simulation of the DØ detector. We calculated the cross section for $W\gamma$ production (with $E_T^\gamma > 10$ GeV and $\Delta R_{l\gamma} > 0.7$) to be $\sigma(p\bar{p} \to W\gamma) = 138^{+51}_{-38}$ (stat) ± 21 (sys) pb compared with the SM prediction of $\sigma(p\bar{p} \to W\gamma) = 112 \pm 10$ pb. Therefore, the observed signal agrees with the

SM prediction (within errors). Fig. 7 shows the kinematic distributions for the observed candidate events together with the SM signal prediction plus the sum of the estimated backgrounds. The shapes of these distributions show no deviations from the expectations. To set limits on the $WW\gamma$ vertex coupling parameters, we used a binned maximum likelihood fit to the photon E_T distribution. Fig. 8 shows the 68% and 95% confidence level (CL) limits in the $\Delta\kappa^0$–λ^0 plane, where we have used a form factor scale of $\Lambda = 1.5$ TeV. Varying only one coupling at a time we find the following limits at the 95% CL:

$$-1.6 < \Delta\kappa^0 < 1.8 \qquad (\text{for } \lambda^0 = 0)$$
$$-0.6 < \lambda^0 < 0.6 \qquad (\text{for } \Delta\kappa^0 = 0).$$

The possibility of a minimal U(1)-only coupling ($\kappa=\lambda=0$) indicated by the star in Fig. 8 is ruled out at the 88% CL.

The CDF $W\gamma$ analysis, described in [15], also sets limits on the $WW\gamma$ vertex couplings. These limits are shown in Fig. 9, together with the DØ limits described above.
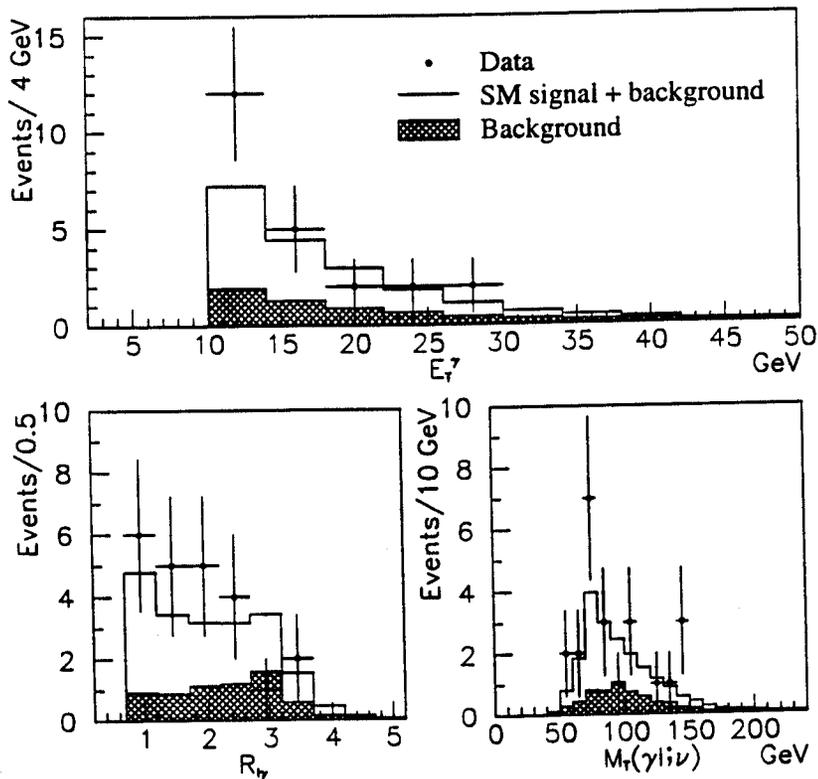
Fig. 7.   Distribution of photon transverse energy E_T^γ (top), $\Delta R_{l\gamma}$ (left) and transverse cluster mass $M_T(l\gamma;\nu)$ for the $W(e\nu)\gamma + W(\mu\nu)\gamma$ combined sample. The points are data. The shaded areas represent the estimated background and the solid histograms are the expected signal from the Standard Model plus the estimated background.
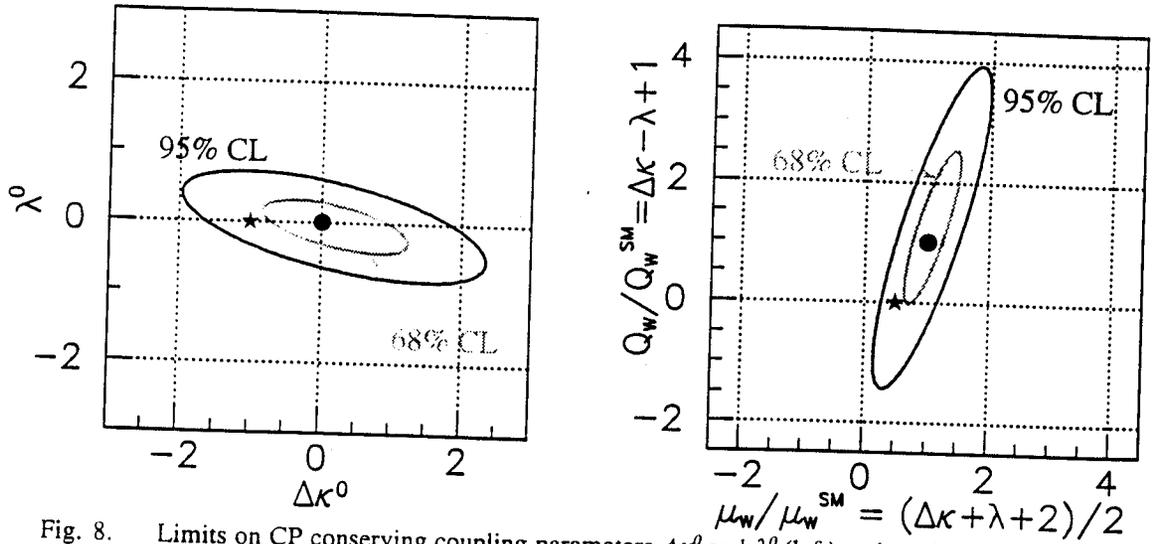
Fig. 8. Limits on CP conserving coupling parameters $\Delta\kappa^0$ and λ^0 (left) and on the magnetic dipole μ_W and electric quadrupole Q_W moments. The ellipses represent the 68% and 95% CL exclusion contours. ● represents the Standard Model values, while ★ indicates the U(1)-only coupling of the W boson to the photon, $\Delta\kappa=-1$ and $\lambda=0$ ($\mu_W=e/2m_W$ and $Q_W=0$).
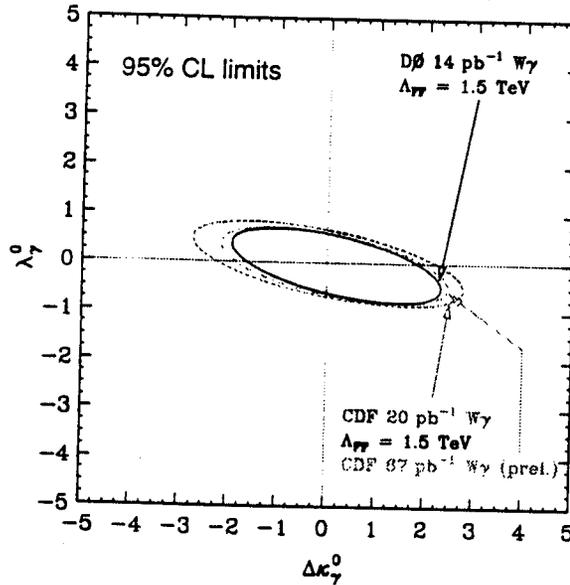

Fig. 9. Limits on the $WW\gamma$ anomalous coupling parameters from DØ and CDF.

5. Zγ Production

At the Tevatron $Z\gamma$ production can be used to test for the possibility of non-zero $ZZ\gamma$ and $Z\gamma\gamma$ couplings. The SM $Z\gamma$ production processes are shown in Fig. 10 (a)-(c). These are analagous to the u- and t-channel and inner bremsstrahlung processes in $W\gamma$ prduction. For non-SM $ZZ\gamma$ or $Z\gamma\gamma$ couplings the diagram of Fig. 10 (d) results in an increased cross section and an enhacement of events with high-E_T photons.
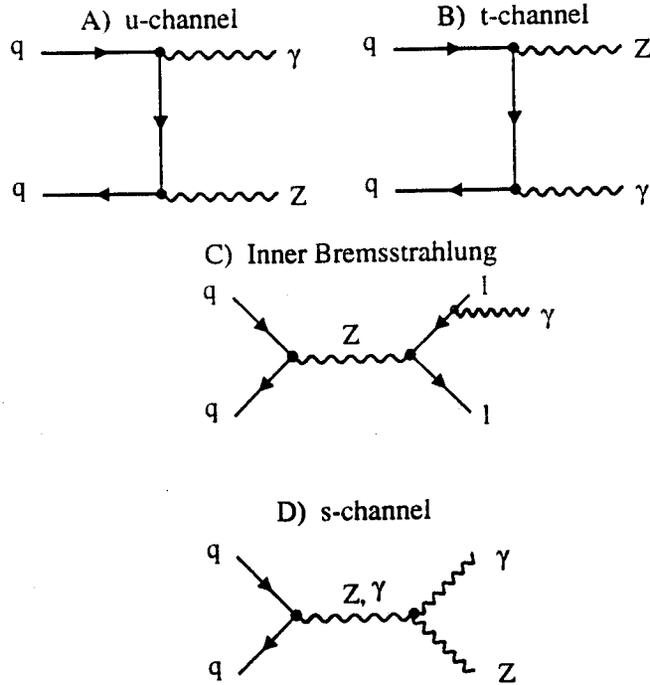
Fig. 10.   Feynman diagrams contributing to the process $p\bar{p} \rightarrow l^+l^-\gamma$.

We searched for $Z\gamma$ events in which the Z decays into e^+e^- or $\mu^+\mu^-$. The $ee\gamma$ sample was selected from a trigger requiring two isolated EM clusters, each with $E_T > 20$ GeV. One electron is required to pass the standard electron quality cuts and the second electron must pass all these cuts except the requirement of a matching track in the drift chambers. Both electrons were required to have $E_T > 25$ GeV. The photon must have $E_T > 10$ GeV and be separated from both electrons by $\Delta R_{l\gamma} > 0.7$. These selection criteria resulted in four $ee\gamma$ candidates and two $\mu\mu\gamma$ candidates.

The backgrounds were from (i) Z + jet(s) production where one of the jets fakes a photon or an electron (the latter case corresponds to the $ee\gamma$ signature if, additionally, one of the electrons from the $Z \rightarrow ee$ decay is not detected in a tracking chamber); (ii) QCD multijet production with jets being misidentified as electrons or photons; (iii) $\tau\tau\gamma$ production followed by the decay of each τ to $l\bar{\nu}_l\nu_\tau$. Backgrounds (i) and (ii) were calculated from data using the misidentification probabilities $P(\text{jet} \rightarrow e)$ and $P(\text{jet} \rightarrow \gamma)$

estimated from multijet events as described above. The $\tau\tau\gamma$ background was estimated using the ISAJET Monte Carlo event generator followed by a full GEANT simulation of the DØ detector.

After subtracting the backgrounds, the signal is $3.57^{+3.15}_{-1.91} \pm 0.06$ events for the $ee\gamma$ channel and $1.95^{+2.62}_{-1.29} \pm 0.01$ events for the $\mu\mu\gamma$ channel, where the first error is due to Poisson statistics and the second is due to the systematic uncertainty of the background estimate.

To set limits on anomalous $ZZ\gamma$ and $Z\gamma\gamma$ couplings we used a fit to the photon E_T distribution, as described above for the $W\gamma$ analysis. Figure 11 shows the observed E_T spectrum with the sum of the backgrounds plus SM signal. The latter was obtained using the Baur and Berger event generator [10] combined with a simulation of the DØ detector. The 95% CL limits on the CP-conserving anomalous coupling parameters h_{30}^Z and h_{40}^Z, obtained by varying only one coupling at a time and using a form factor scale of $\Lambda = 500\,\mathrm{GeV}$ are:

$$ZZ\gamma\ \text{coupling:} \qquad -1.8 < h_{30}^Z < 1.8$$
$$-0.5 < h_{40}^Z < 0.5;$$

$$Z\gamma\gamma\ \text{coupling:} \qquad -1.9 < h_{30}^\gamma < 1.9$$
$$-0.5 < h_{40}^\gamma < 0.5.$$

The 95% CL limit contour in the h_{30}^Z–h_{40}^Z plane is shown in Fig. 12 together with the limits from CDF [16] and L3 [17]. The L3 measurement is based on an analysis of $Z \rightarrow \nu\bar{\nu}\gamma$. At the LEP energy the sensitivity to h_{40}^γ is less than that to h_{30}^Z. At the Tevatron the anomalous couplings are probed at higher $\sqrt{\hat{s}}$, and because the helicity amplitude contributions grow like $(\sqrt{\hat{s}}/M_Z)^5$ for h_{40}^γ and $(\sqrt{\hat{s}}/M_Z)^3$ for h_{30}^Z, the Tevatron measurements are more sensitive to h_{40}^γ.
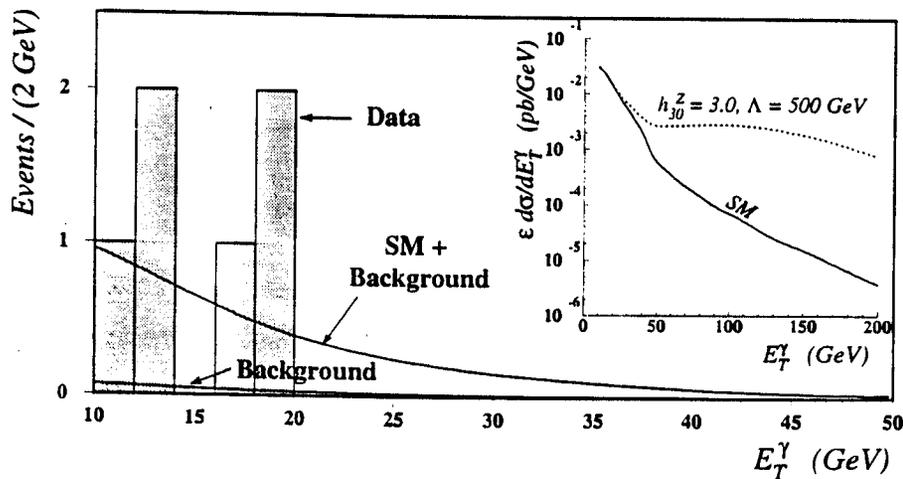
Fig. 11. Photon E_T distribution for the $Z(ee)\gamma + Z(\mu\mu)\gamma$ candidate events. The sum of the backgrounds plus SM signal is also shown. The inset shows the enhancement of high p_T photons for anomalous couplings.
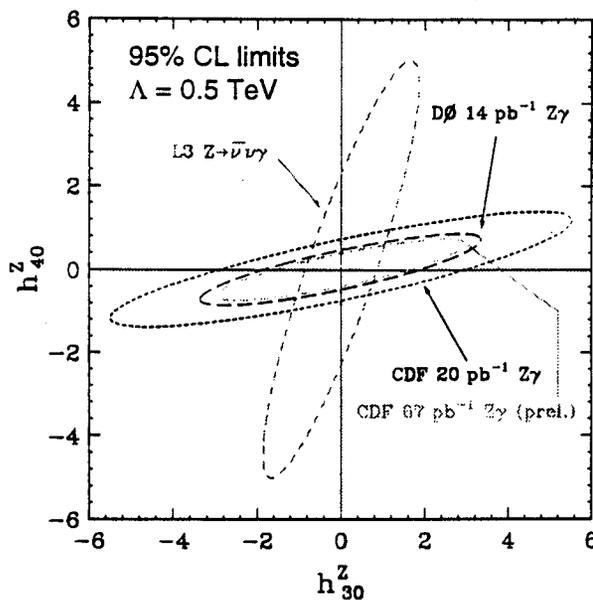
13

Fig. 12. Limits on the anomalous $ZZ\gamma$ coupling parameters from DØ, CDF and L3.

6. *WW* and *WZ* Production

We have searched for *WW* and *WZ* production using two decay modes: (a) $WW \to l\nu\, l\nu$, or the "dilepton" mode and (b) $WW, WZ \to l\nu\, q\bar{q}$, or the "lepton plus jets" mode. In the dilepton analysis [18] we search in the ee, $\mu\mu$ and $e\mu$ channels, requiring two high p_T leptons and missing E_T greater than 20 GeV. One event passes the selection criteria (an ee event). The SM prediction for the *WW* signal, based on a cross section of 9.5 pb [19] is 0.47 ± 0.07 events. We set an upper limit on the cross section for $p\bar{p} \to W^+W^- + X$ of 87 pb at the 95% CL, estimated based on one signal event including subtraction of the total estimated background of 0.56 ± 0.13 events.

The *W* pair production process is sensitive to the *WW*γ *and* *WWZ* couplings, since the s-channel propagator can be a γ or *Z*. We set limits on the anomalous coupling parameters, assuming that $\Delta\kappa_Z = \Delta\kappa_\gamma$, $\lambda_Z = \lambda_\gamma$. The limits obtained from the obsereved cross section limit and the theoretical cross section as a function of $\Delta\kappa$ and λ are shown in Fig. 14.

In the *preliminary* lepton plus jets analysis we search for $WW, WZ \to l\nu jj$ candidate events containing a $W \to e\nu$ decay ($E_T^e > 25$ GeV, $\not{E}_T > 25$ GeV forming a transverse mass > 40 GeV) and two jets consistent with $W \to jj$ or $Z \to jj$. The candidate events were required to contain at least two jets with $E_T^j > 25$ GeV and have a dijet mass of $50 < m_{jj} < 110$ GeV/c^2 (the largest mass was taken if the event had more than two jets). A cone algorithm with a radius $R = 0.3$ was used to reconstruct jets. This small cone size minimizes the probability for two jets from the *W* or *Z* boson to merge into one cluster in the calorimeter, especially for high p_T *W* and *Z* bosons. Figure 13 shows the observed p_T

distribution of the ev system. As shown, the data are dominated by background, mainly from (i) W+≥2jets events with $W \to ev$ and (ii) multijet production where one jet was misidentified as an electron and there was significant (mismeasured) missing E_T.

At large values of the $p_T(W \to ev)$ the backgrounds are relatively small and it is in this region where anomalous couplings would enhance the cross section, as shown in the lower plot of Fig. 13. Therefore we performed a binned likelihood fit to the p_T^w spectrum above $p_T^w > 25$ GeV. The results, assuming the WWZ and $WW\gamma$ coupling parameters are equal (see section 3), are shown in Fig. 14. At the 95% CL, for $\Lambda = 1.0$ TeV, we obtain

$$-0.9 < \Delta\kappa^0 < 1.1 \qquad \text{(for } \lambda^0 = 0)$$
$$-0.7 < \lambda^0 < 0.7 \qquad \text{(for } \Delta\kappa^0 = 0).$$

Note that the limits on $\Delta\kappa$ from this channel are tighter than those from the $W\gamma$ channel, but note that we assumed $\Delta\kappa_z=\Delta\kappa_\gamma$.
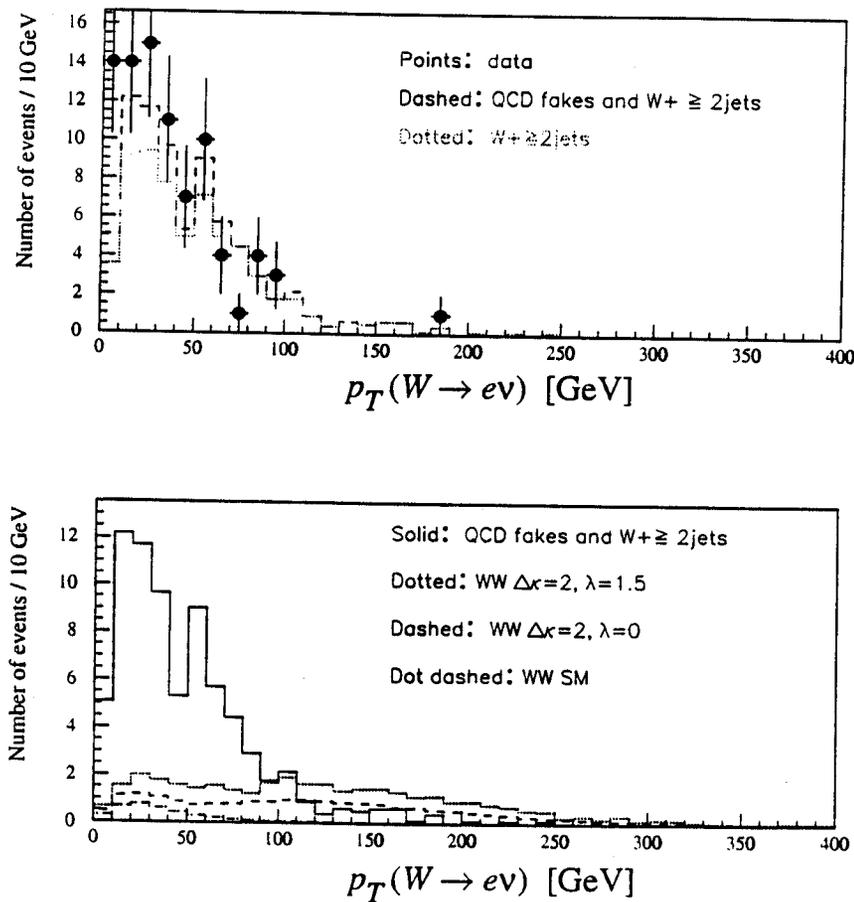
Fig. 13. p_T of the ev system: data (points), $W + \geq 2$ jets background (dotted) and total background (dashed). In the second plot, the total background is compared with the predicted signal for anomalous couplings and shows the enhancement of the signal at high p_T.
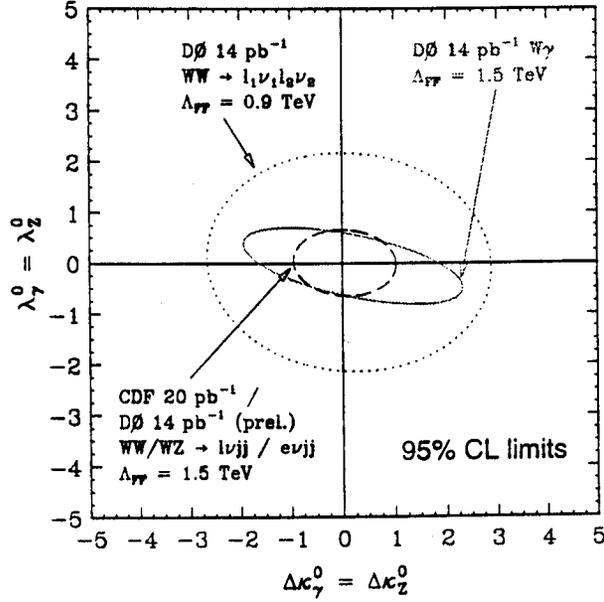
Fig. 14. Summary of limits on the anomalous WWV coupling parameters $\Delta\kappa$ and λ assuming $\Delta\kappa_Z=\Delta\kappa_\gamma$ and $\lambda_Z=\lambda_\gamma$

7. Conclusions

Recent analyses of data based on the production of W and Z bosons using ≈ 12 pb^{-1} of data collected at the Fermilab Tevatron have resulted in considerable improvements in the measurement of the properties of the W boson. As an example, the indirect measurement of the W boson width is $\Gamma(W) = 2.062 \pm 0.059$ GeV (world average), corresponding to a precision of 3% on $\Gamma(W)$.

New studies of the physics of electroweak gauge boson pair production have also been undertaken. The production of $W\gamma$ and $Z\gamma$ events is in agreement with the predictions of the Standard Model, within the experimental sensitivity. These measurements allow limits to be set on anomalous electroweak gauge boson couplings. Searches for WW and WZ production are also used to set limits. The current 95% CL limits on the $WW\gamma$ coupling parameters from the $W\gamma$ channel are:

$$-0.9 < \Delta\kappa^0 < 1.1 \qquad \text{(for } \lambda^0 = 0\text{)}$$
$$-0.7 < \lambda^0 < 0.7 \qquad \text{(for } \Delta\kappa^0 = 0\text{)}.$$

and the limits on the $ZZ\gamma$ coupling parameters are ($\Lambda = 500$ GeV):

$$-1.8 < h_{30}^Z < 1.8 \qquad \text{(for } h_{40}^Z = 0\text{)}$$
$$-0.5 < h_{40}^Z < 0.5 \qquad \text{(for } h_{30}^Z = 0\text{)}.$$

16

It is important to note that the measurements described in this paper are based on Run 1a data only. Analyses of the data from the complete Run 1 (≈ 100 pb^{-1}) will soon be completed and will lead to increases in the precision of these measurements. The upgraded DØ and CDF detectors will begin running at the Tevatron in 1999 collecting data sets of >2 fb^{-1} in the first few years. As an example, the W width is expected to be measured with an error of ± 40 MeV from Run 1 and ± 20 MeV assuming an integrated luminosity of 10 fb^{-1}. With 10 fb^{-1} of data the WWV vertex ($V=\gamma,Z$) coupling parameters can be tested at the level of $\approx 10\%$, and the $ZV\gamma$ vertex couplings at the level of 10^{-2}–10^{-3}. Complimentary tests of the anomalous couplings will also come from LEP II.

Acknowledgments

References

[1]   UA1 Collaboration, G. Arnison *et al.*, Phys. Lett. **122B**, 103 (1983); **126B**, 398 (1983); UA2 Collaboration, M. Banner *et al.*, Phys. Lett. **122B**, 476 (1983); P. Bagnaia *et al.*; Phys. Lett. **129B**, 130 (1983).

[2]   DØ Collaboration, S. Abachi *et al.*, Nucl. Instr. and Methods **A338**, 185 (1994).

[3]   DØ Collaboration, S. Abachi *et al.*, Phys. Rev. Lett. **75**, 1456 (1995).

[4]   F. Carminati *et al.*,"GEANT Users Guide" CERN Program Library, December 1991 (unpublished).

[5]   H. L. Lai *et al.*, Phys. Rev. D **51**, 4763 (1995)

[6]   R. Hamberg, W. L. van Neerven and T. Matsuura, Nucl. Phys. **B359**, 343 (1991).

[7]   Particle Data Group, L. Montanet *et al.*, Phys. Rev. D **50**, 1173 (1994).

[8]   J. L. Rosner, M. P. Worah and T. Takeuchi, Phys. Rev. D **49**, 1363 (1994).

[9]   K. Hagiwara, R.D. Peccei and D. Zeppenfeld, Nucl. Phys. **B282**, 253 (1987).

[10]   U. Baur and E.L. Berger, Phys. Rev. D **47**, 4889 (1993)

[11]   U. Baur and E.L. Berger, Phys. Rev. D **41**, 1476 (1990).

[12]   DØ Collaboration, S. Abachi *et al.*, Phys. Rev. Lett. **75**, 1034 (1995).

[13]   F. Paige and S. Protopopescu, BNL Report no. BNL–38034, 1986 (unpublished), release V6.49.

[14]   U. Baur and D. Zeppenfeld, Nucl. Phys. **B308**, 127 (1988).

[15]   CDF Collaboration, F. Abe *at al.*, Phys. Rev. Lett. **74**, 1936 (1995).

[16]   CDF Collaboration, F. Abe *at al.*, Phys. Rev. Lett. **74**, 1941 (1995).

[17]   L3 Collaboration, M. Acciarri *et al.*, Phys. Lett. B346, 190 (1995).

[18]   DØ Collaboration, S. Abachi et al., Phys. Rev. Lett. **75**, 1023 (1995).

[19]   J. Ohnemus, Phys. Rev. D **44**, 1403 (1991).

Electroweak Physics Results from the DØ Experiment at Fermilab

John A. Ellison

University of California, Riverside

(for the DØ Collaboration)

Outline of this talk:

- Overview of the DØ detector

- W and Z cross sections and the inclusive width of the W

- Measurement of the W mass

- Diboson production ($W\gamma$, $Z\gamma$, W^+W^-) and the trilinear vector boson couplings

The DØ Detector

- Approved in 1984

- Fermilab Tevatron $p\bar{p}$ collider $\sqrt{s} = 1.8$ TeV

- First Collider Run ("Run 1A") 1992-93

  $\rightarrow \approx 14$ pb^{-1} recorded to tape

- Second Collider Run ("Run 1B") 1993-95

  $\rightarrow \approx 85$ pb^{-1} recorded to tape

- Most of the analyses presented in this talk are based only on the Run 1A data sample – *some* preliminary data from Run 1B will be shown

The DØ Detector
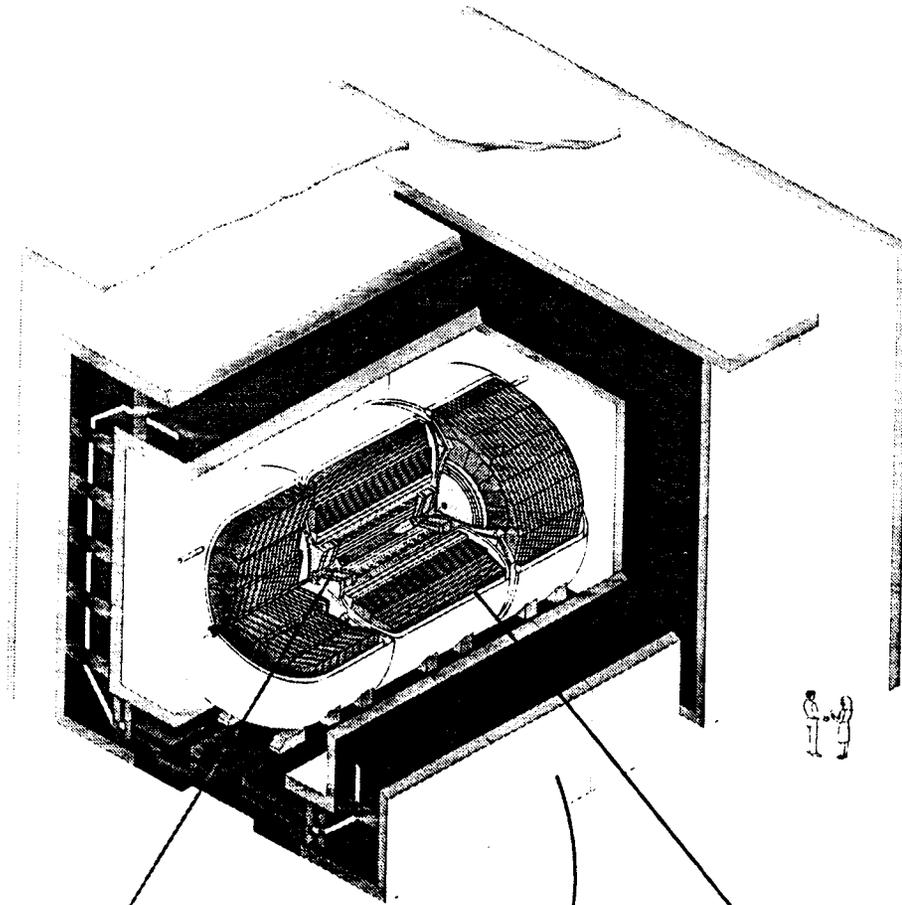
TRACKING

$\sigma(z \text{ vertex}) = 6$ mm
$\sigma(r\phi) = 60\ \mu$m   (VTX)
       $= 180\ \mu$m (CDC)
       $= 200\ \mu$m (FDC)

MUON

$|\eta| < 3.3$

$\dfrac{\delta p}{p} = 0.2 \oplus 0.01p$

CALORIMETRY

$|\eta| < 4$

$\Delta\eta \times \Delta\phi = 0.1 \times 0.1$

$\sigma(EM) = 15\% / \sqrt{E}$

$\sigma(HAD) = 50\% / \sqrt{E}$

$$\eta = -\ln \tan(\theta/2)$$

Particle Identification

1) Electrons and Photons ($|\eta| < 1.1$ or $1.5 < |\eta| < 2.5$)

- Longitudinal and transverse shower shape in EM calorimeter consistent with that expected for an electron

- EM cluster isolation

- Track match in central or froward drift chambers (electrons)

2) Muons ($|\eta| < 1.7$)

- Good quality isolated muon track

- Track match in CD and energy deposition in calorimeter consistent with minimum ionizing particle

- Impact parameter and timing cuts to suppress cosmic ray events

3) Neutrinos

- Missing E_T

4) Jets ($|\eta| < 4.0$)

- Cone algorithm with $\Delta R \equiv \sqrt{\Delta\eta^2 + \Delta\phi^2} = 0.7$

W and Z production cross sections

Channel	$W \rightarrow e\nu$	$Z \rightarrow ee$	$W \rightarrow \mu\nu$	$Z \rightarrow \mu\mu$
p_T^1 $(p_T^2, \not{E}_T)$ (GeV)	25.25	25.25	20.20	20.15
Number of candidates	10338	775	1665	77
Backgrounds				
$Z \rightarrow l^+l^-$	0.6 ± 0.1	--	7.3 ± 0.5	0.7 ± 0.2
$W \rightarrow \tau\nu$	1.8 ± 0.1	--	5.9 ± 0.5	--
QCD	3.3 ± 0.5	2.8 ± 1.4	5.1 ± 0.8	2.6 ± 0.8
Cosmic	--	--	3.8 ± 1.6	5.1 ± 3.6
Drell-Yan	--	1.2 ± 0.1	--	1.7 ± 0.3
Total (%)	5.7 ± 0.5	4.0 ± 1.4	22.1 ± 1.9	10.1 ± 3.7
Acceptance (%)	46.0 ± 0.6	36.3 ± 0.4	24.8 ± 0.7	6.5 ± 0.4
Efficiency (%)	70.4 ± 1.7	73.6 ± 2.4	21.9 ± 2.6	52.7 ± 4.9
$\int L dt$ (pb^{-1})	12.8 ± 0.7	12.8 ± 0.7	11.4 ± 0.6	11.4 ± 0.6
$\sigma \cdot B$ (nb)	**2.36**	**0.218**	**2.09**	**0.178**
$\pm$stat	± 0.02	± 0.008	± 0.06	± 0.022
$\pm$sys	± 0.07	± 0.008	± 0.22	± 0.021
$\pm$lum	± 0.13	± 0.012	± 0.11	± 0.009

QCD background calculation

- Single electron trigger, no missing E_T requirement

- Select QCD sample by requiring non-isolated electrons

- Select W sample using standard W selection cuts, but with no missing E_T cut
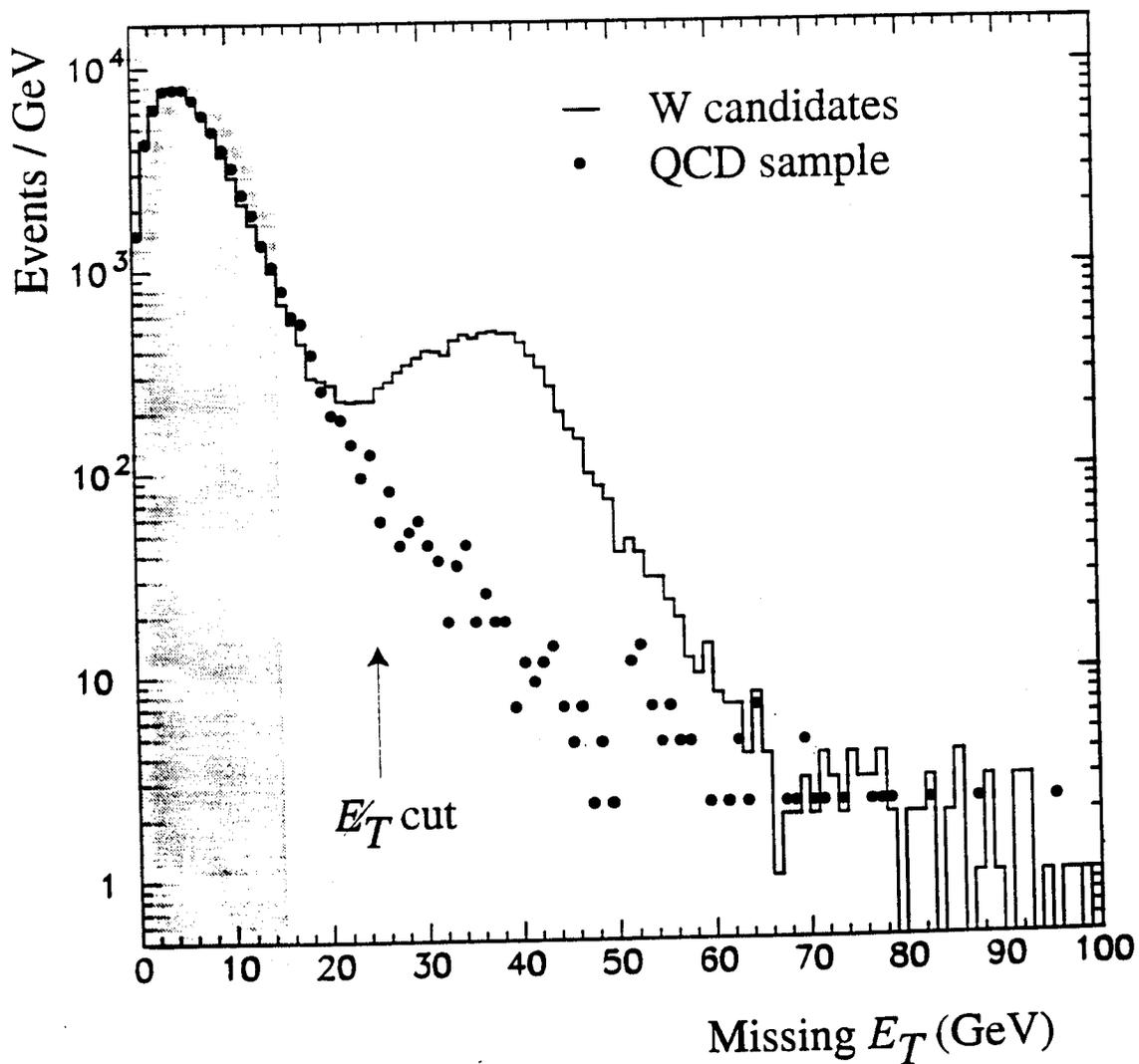
Final *W* and *Z* Candidate Samples
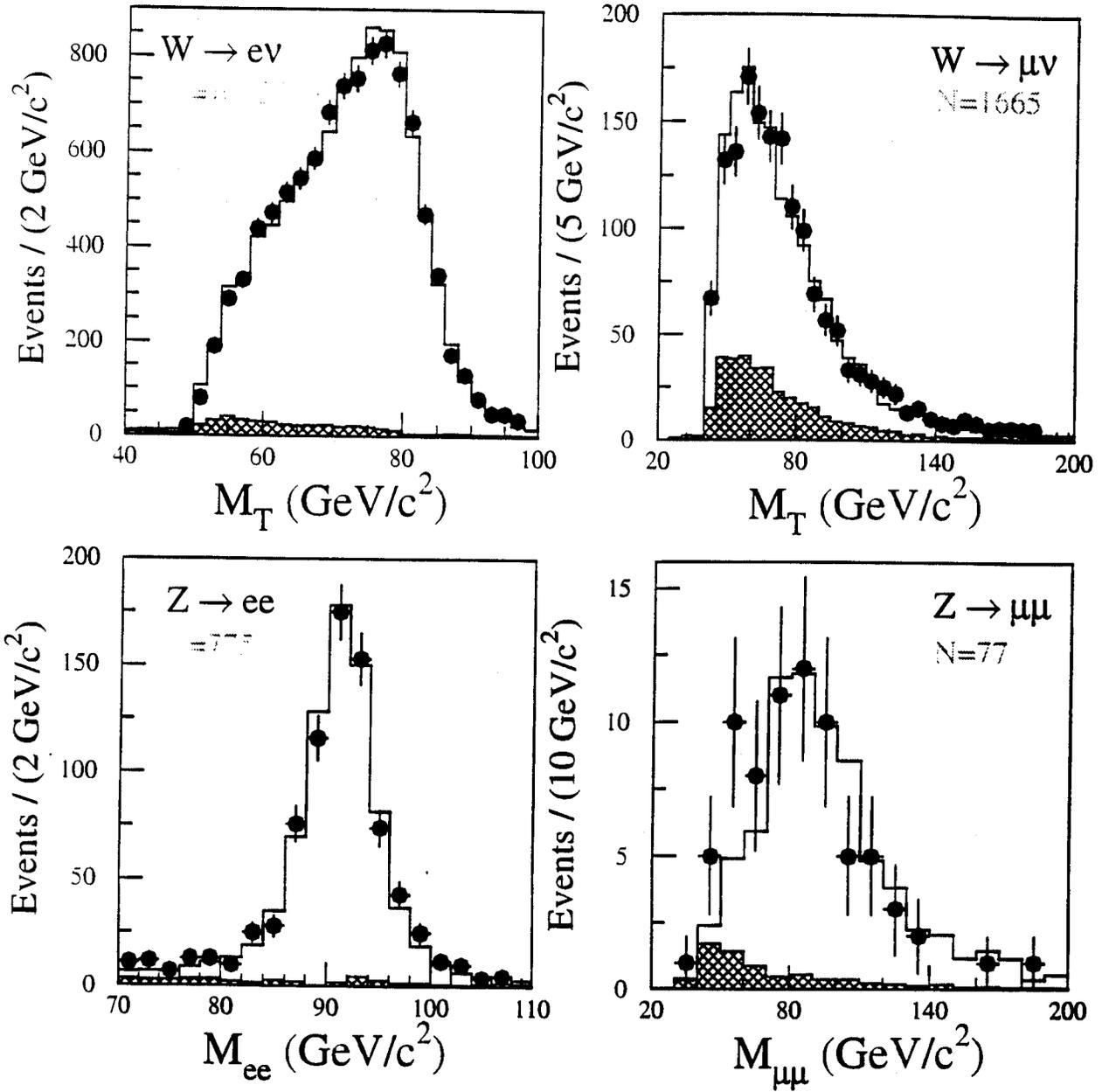
- ● = Observed data

Solid line = MC prediction (signal + background)

Shaded region = estimated background

Transverse Mass $\quad M_T = \sqrt{2 p_T^e p_T^\nu (1 - \cos\theta)}$

DØ and CDF results
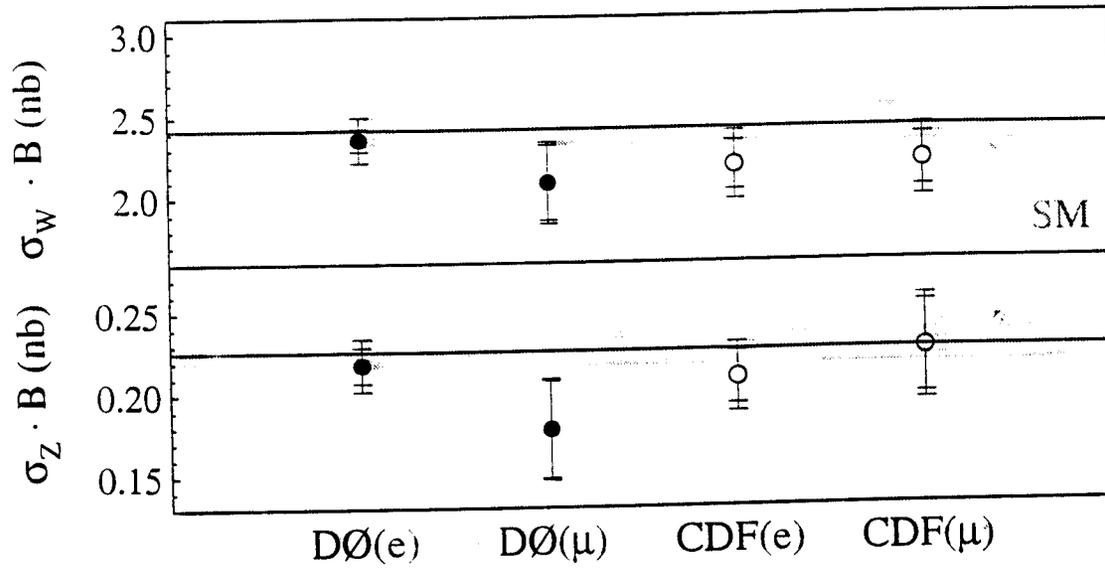
σ·B versus center-of-mass energy
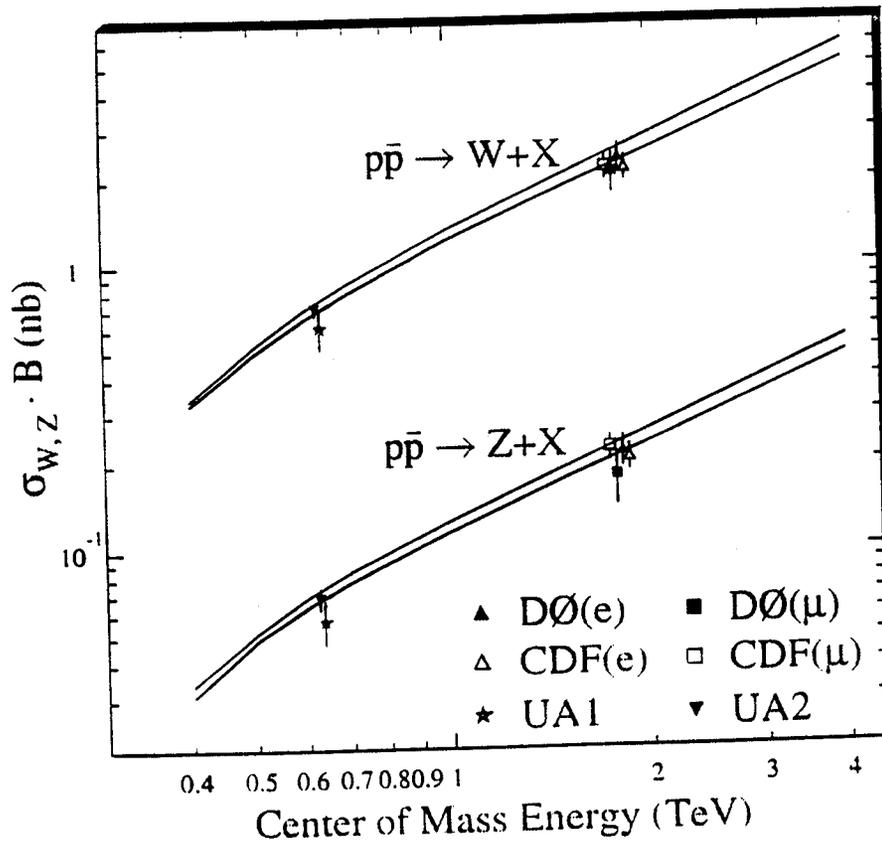
Inclusive Width of the W

$$R = \frac{\sigma_W \cdot B(W \to l\nu)}{\sigma_Z \cdot B(Z \to ll)}; \quad B(W \to l\nu) = \frac{\Gamma(W \to l\nu)}{\Gamma(W)}$$

- Determine R from ratio of measured W and Z $\sigma \cdot B$ values:

$$R\,(e+\mu) = 10.89 \pm 0.49 \; (\text{stat} \oplus \text{sys})$$

- Use theoretical calculation of σ_W / σ_Z and LEP measurement of $B(Z \to ll)$ to obtain $B(W \to l\nu)$:

$$B(W \to l\nu) = 11.02\% \pm 0.49\% \; (\text{expt.}) \pm 0.11\% \; (\text{theory})$$

- Use theoretical calculation of $\Gamma(W \to l\nu)$ to obtain $\Gamma(W)$:

$$\Gamma(W) = 2.044 \pm 0.091 \; (\text{expt.}) \pm 0.017 \; (\text{theory}) \; \text{GeV}$$

Measurements of the Width of the *W*
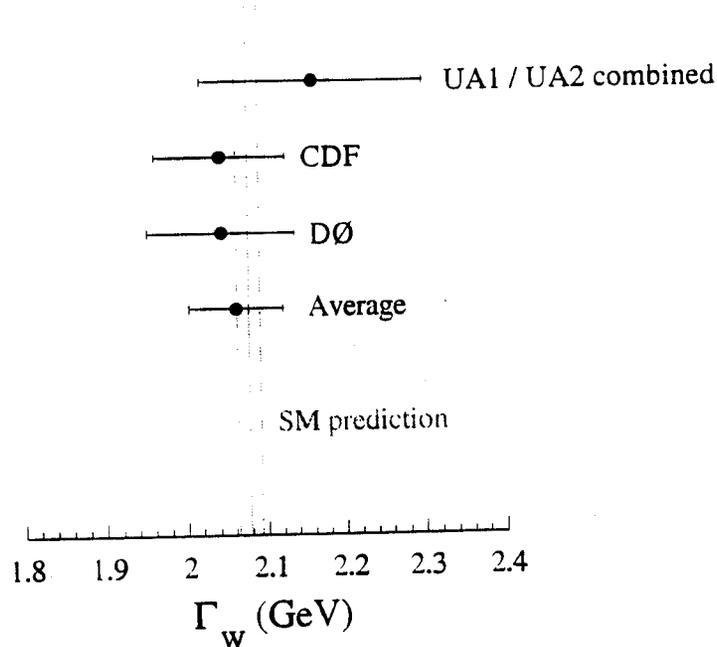
Average of measurements: $\Gamma_W = (2.062 \pm 0.059)$ GeV

Standard Model prediction: $\Gamma_W = (2.077 \pm 0.014)$ GeV

- Measurement of Γ_W can be used to set limits on unexpected decay modes of the *W*, e.g. *W* decays into:

  - supersymmetric charginos and neutralinos
  - heavy quarks

- Comparing the measurements with the SM gives a 95% CL upper limit of 109 MeV on unexpected decays.

W charge asymmetry

- ... asymmetric: quarks carry more ... than quarks
- ... follow proton direction
- ... introduces another (opposite) asymmetry
- Take ... as given, and use lepton charge asymmetry to say "d"
- ... use u(x)/d(x) ratio for $0.007 < x < 0.27$

+y defined in the proton beam direction

W Charge Asymmetry (LO)
W Decay Lepton Charge Asymmetry (LO)

Lepton Cuts
$E_T^e > 25$ GeV
$E_T^\nu > 25$ GeV

Charge Asymmetry

Rapidity

W Asymmetry
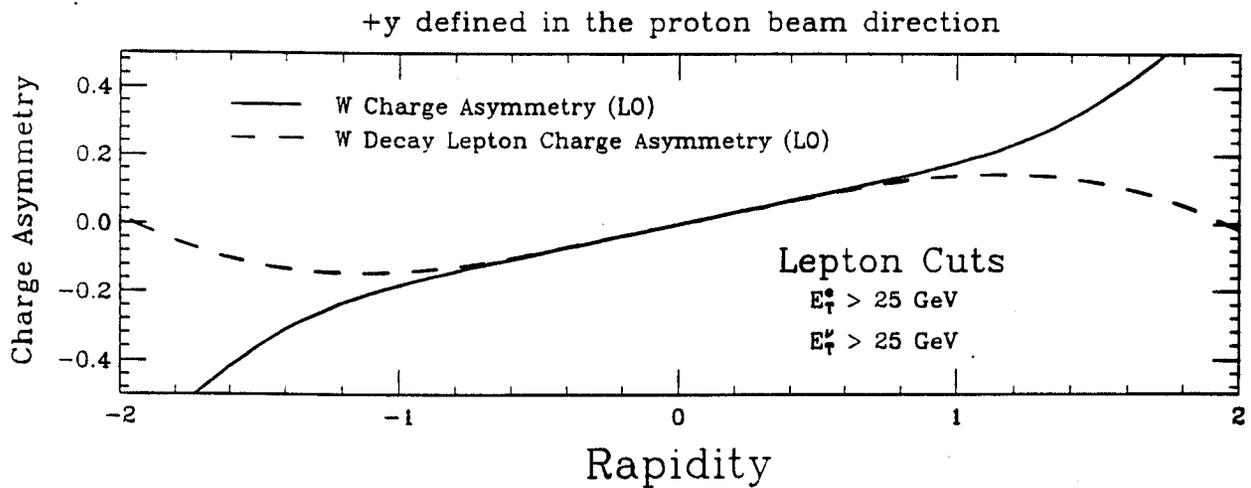
Comparison of D0 and CDF W Asymmetry
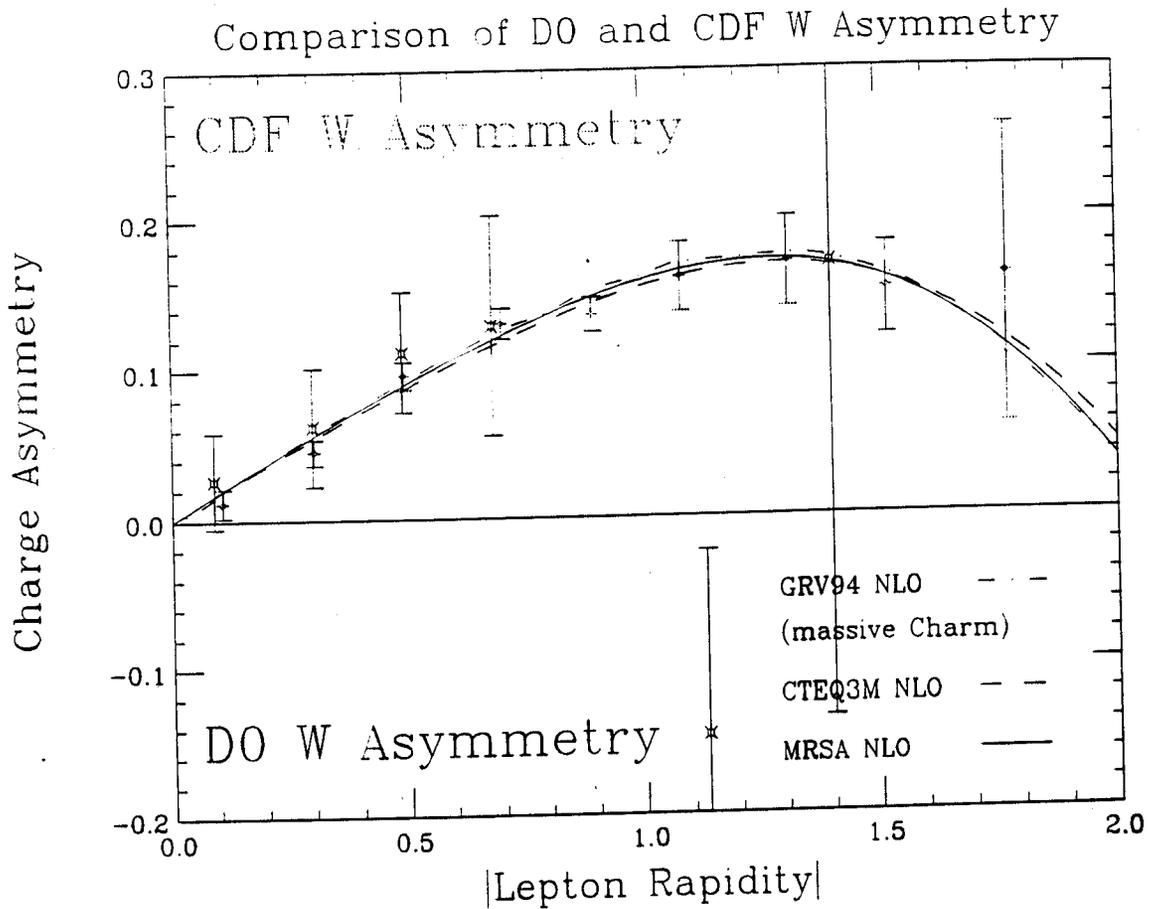
- Run 1A + Run 1B (partial), preliminary:
  - CDF: 67 pb^{-1}
  - D0: 36 pb^{-1} (muons only)
- Theory: "DYRAD" MC, Giele et al, *NP* **B405**, 663.
- Restricts pdf range. Important for W mass determination

W mass analysis

- Preliminary result presented last year was based on a partial data sample from run 1A:

$$M_W = 79.86 \pm 0.16(\text{stat}) \pm 0.17(\text{sys}) \pm 0.26(\text{scale})$$

- Our analysis is still in progress – we have made major improvements in our understanding of the detector simulation:

    - resolutions

    - Missing E_T trigger efficiency

    - Biases from detector effects such as zero suppression and clustering algorithms

- We have, in addition, begun using:

    - $d^2\sigma/dp_T^W dy$ distribution based on resummed calculation of Yuan and Ladinsky

    - Radiative decays (Berends and Kleiss)

W mass measurement technique

- Measure electron momentum and p_T of recoil system

- Neutrino p_T obtained from $p_T^\nu = -p_T^e - p_T^{had}$
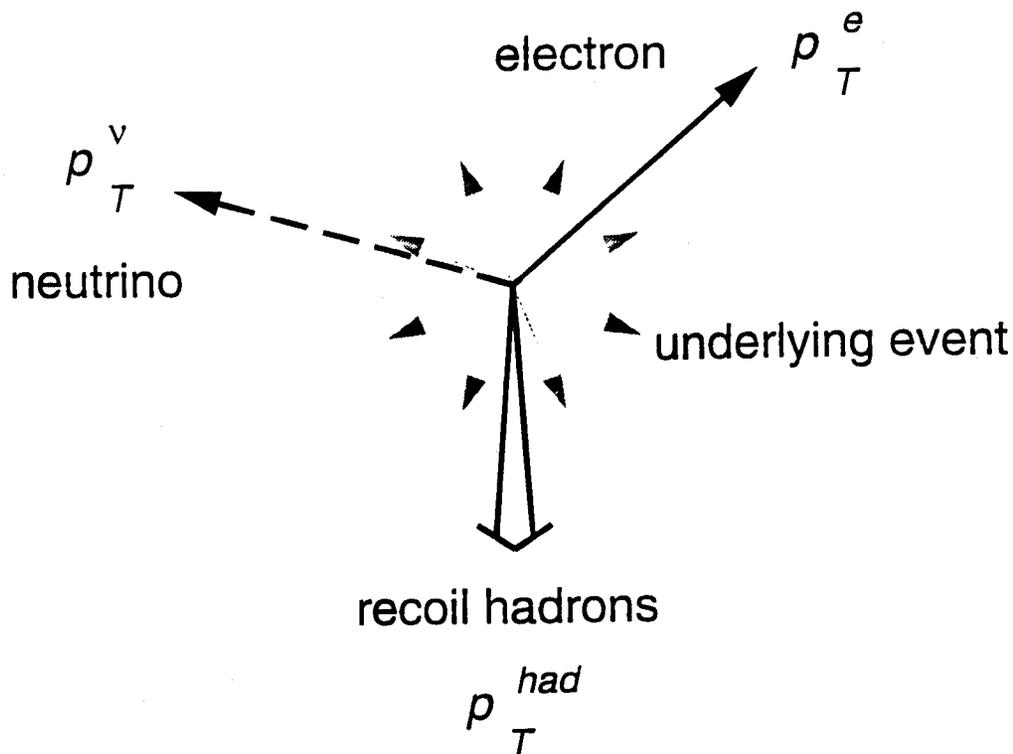
- Calculate transverse mass $M_T = \sqrt{2 p_T^e p_T^\nu (1 - \cos\theta)}$

- Use fast MC to model $W \to e\nu$ events and add backgrounds

- Generate M_T spectra for various M_W values

- Fit MC M_T spectra to data to obtain best fit M_W value using the maximum likelihood method

W mass measurement – errors

- Summary of errors – DØ preliminary (Glasgow 94):

	Error (MeV)
Energy scale	260
Resolution	70
Background	30
Fitting	30
PDF	70
p_T^w and und. evt.	120
Width	20
Total systematic	307
Statistcal	160
Total (stat + sys)	346

Comments:

- The statistical error for our *complete* run 1A data sample will be reduced to approximately 150 MeV

- The energy scale error has been reduced to approximately 170 MeV

EM Energy Scale Calibration

- Use collider data: $Z \rightarrow ee$, $J/\psi \rightarrow ee$ and $\pi^0 \rightarrow \gamma\gamma \rightarrow ee\,ee$

- Assume linear relation of form $E_{obs} = \delta + \alpha E_{true}$

$\underline{Z \rightarrow ee:}$

$$m_{obs} = \alpha m_{true} + f\delta$$

$$f = \frac{(E_1^e + E_2^e)(1 - \cos\theta)}{m_{obs}}$$

$f \sim 2$ $\qquad\qquad$ $f \sim 1.5$

$E_1 \sim 45$ GeV $\qquad\qquad$ $E_1 \sim 70$ GeV

$\theta \sim 180°$

$E_2 \sim 45$ GeV $\qquad\qquad$ $E_2 \sim 70$ GeV
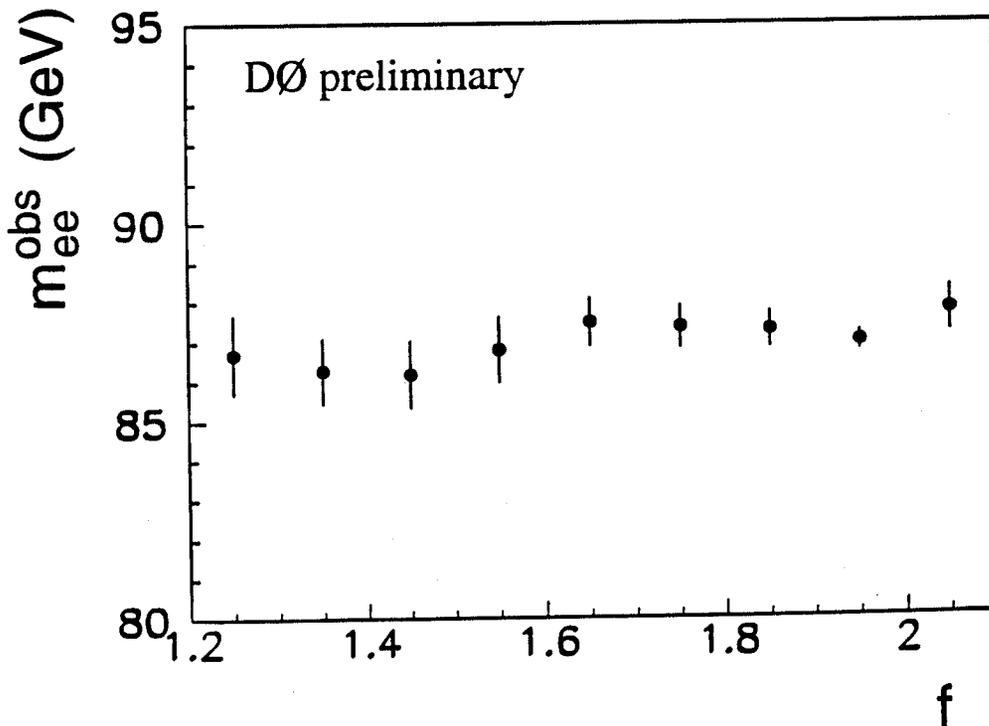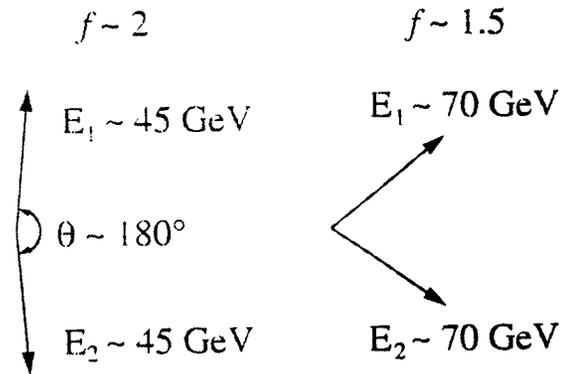
EM Energy Scale – offset and slope

D0 preliminary

$$E_{obs} = \delta + \alpha E_{true}$$

$Z \to ee$

$\pi^0 \to \gamma\gamma$ $\quad$ $J/\psi \to ee$

D0 preliminary
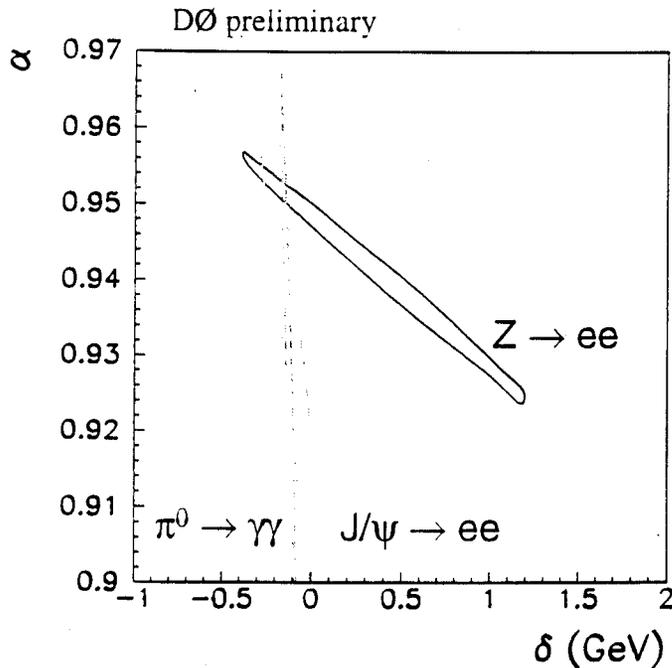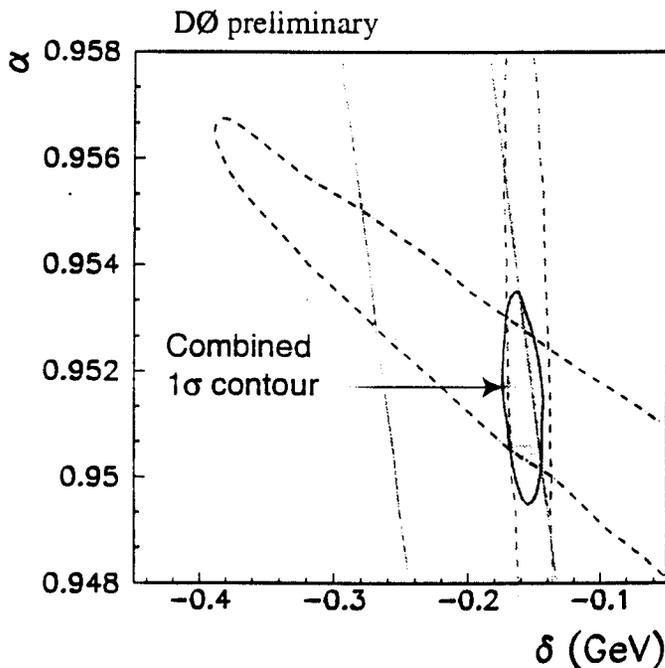
$\alpha \approx 0.95$

$\delta = -0.16 \pm 0.016$ (stat) GeV

Combined
1σ contour

Systematics:
  – assumption of linearity
  – modelling of underlying
    event in simulation

$\delta = -0.16 \,{}^{+0.034}_{-0.210}$ (stat+sys) GeV

- Error due to uncertainty in $\delta \approx 20$ MeV
- Final error due to energy scale uncertainty ≈ 170 MeV
  (dominated by statistical error on M_Z)

W mass error

- Final error due to energy scale $\approx$ 170 MeV (DØ preliminary)

- Expect to have final result for M_W soon

Future measurements of M_W

scaling of W−mass error
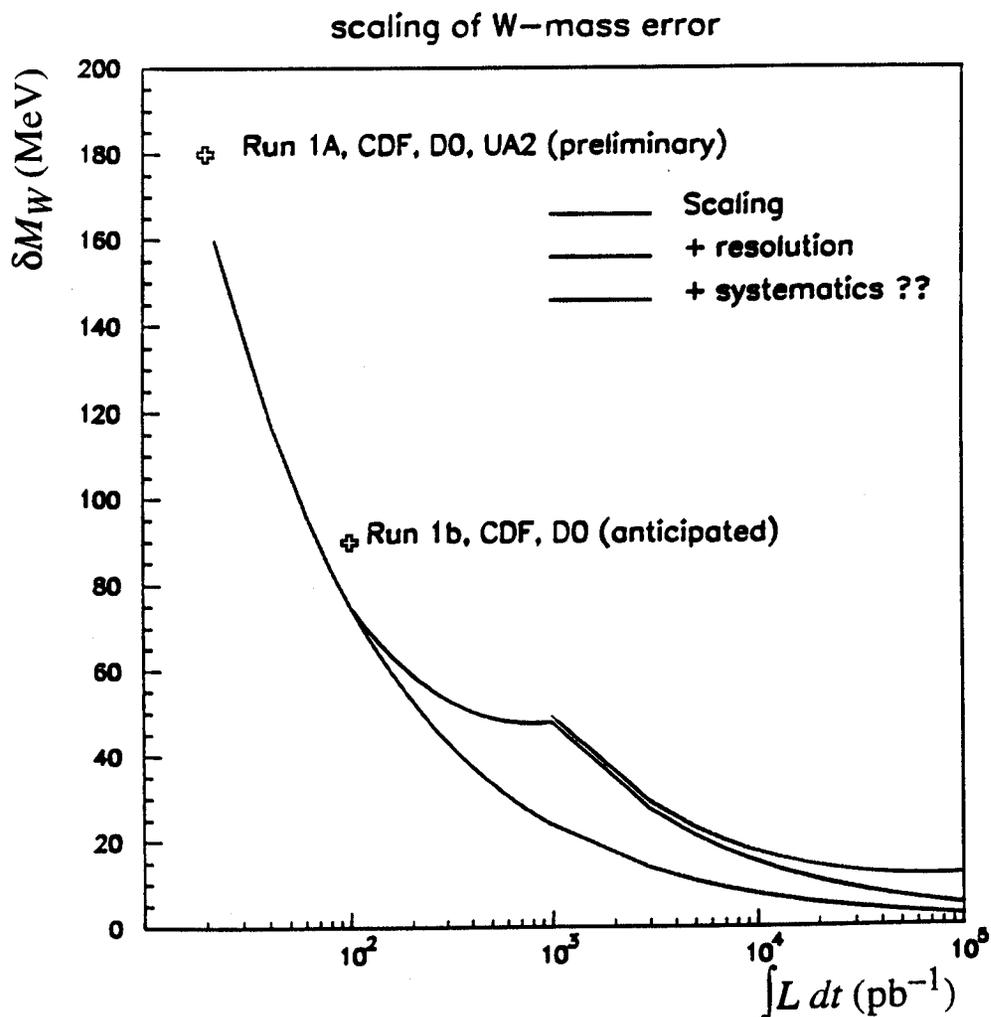
Direct Measurement of the W, Z and γ self-couplings

- Demonstrate agreement with Standard Model

- Use as probe of new physics:

1) Radiative corrections,   e.g. $WW\gamma$

| SM | SM Correction | Non-SM correction |
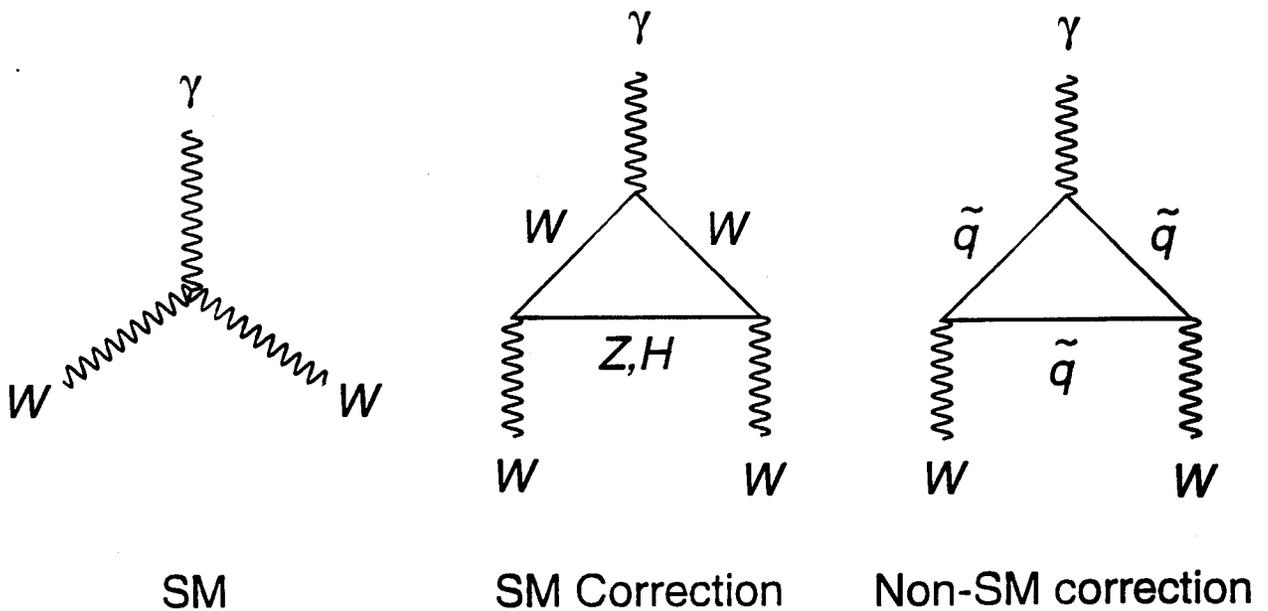
2) Compositeness of the W, Z bosons

$W\gamma$ production

A) u-channel

B) t-channel

C) s-channel

D) Inner Bremsstrahlung
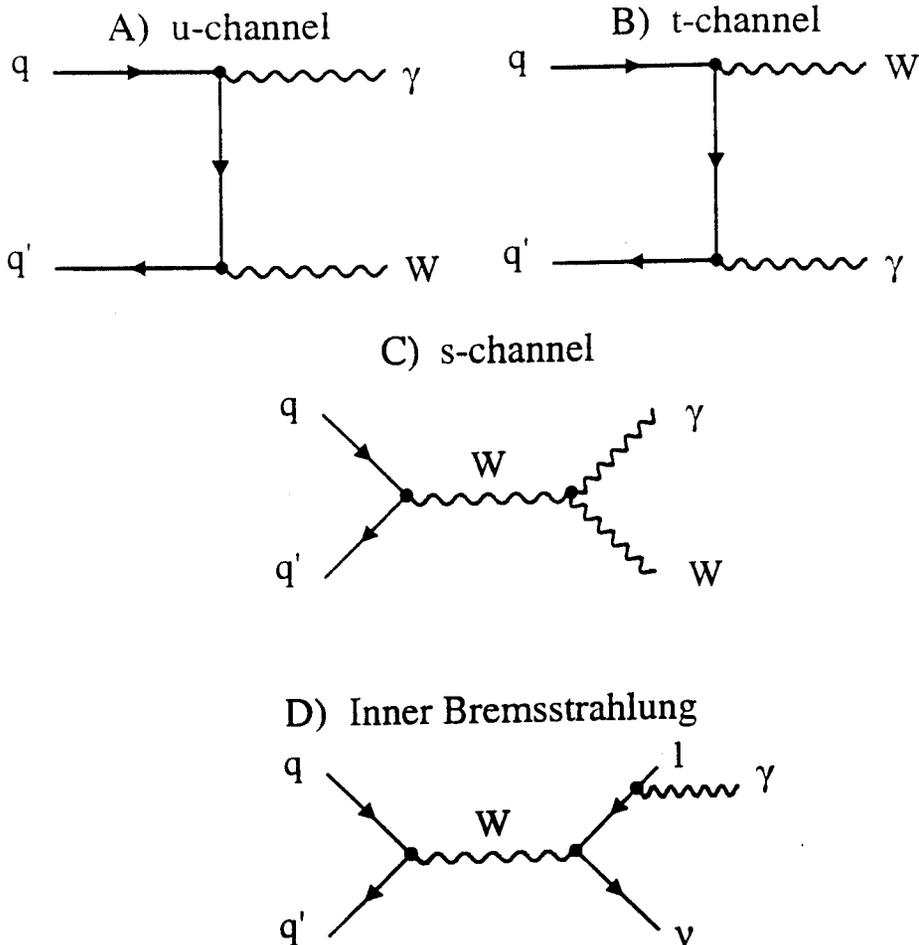
- The s–channel diagram probes the $WW\gamma$ coupling

- Radiative decays can be suppressed by imposing a cut on the photon–lepton angular separation and further by requiring the $(l, \gamma; \nu)$ transverse mass to be $> M_W$

- Radiation zero occurs at

$$\cos\theta^*_{q\gamma} = 1 - \frac{2Q_{\bar{q}}}{Q_W} = \begin{cases} -\frac{1}{3} & u\bar{d} \to W^+\gamma \\ +\frac{1}{3} & d\bar{u} \to W^-\gamma \end{cases}$$

The WWγ and WWZ vertices

Assume electromagnetic gauge
invariance and invariance under
Lorentz, C and P transformations

$$V = \gamma, Z$$
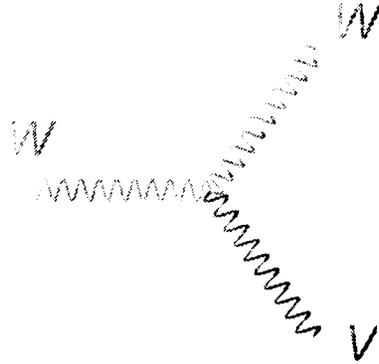
To quantify experimental sensitivity –
parameterize WWV in terms of the effective Lagrangian:

$$i\mathcal{L}_{eff}^{WWV} = g_{WWV}\left[g_1^V(W_{\mu\nu}^\dagger W^\mu - W^{\dagger\mu}W_{\mu\nu})V^\nu + \kappa_V W_\mu^\dagger W_\nu V^{\mu\nu} + \frac{\lambda_V}{m_W^2}W_{\rho\mu}^\dagger W_\nu^\mu V^{\nu\rho}\right]$$

where $g_{WWV} = \begin{cases} -e & V = \gamma \\ -e\cot\theta_W & V = Z \end{cases}$

$$g_1^V, \quad \kappa_V, \quad \lambda_V \quad \text{are dimensionless couplings}$$

In the SM at tree level,

$$g_1^V = 1, \quad \kappa_V = 1, \quad \lambda_V = 0$$

Assume coupling of W to Z and to γ are equal $->$ 2 parameters

$$\kappa_\gamma = \kappa_Z = \kappa \qquad (\text{or } \Delta\kappa \equiv \kappa - 1)$$
$$\lambda_\gamma = \lambda_Z = \lambda$$

$$\boxed{\textit{Physical significance of the coupling parameters}}$$

Consider the $WW\gamma$ vertex
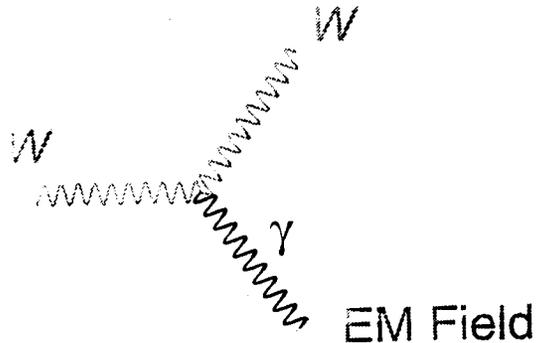
The coupling parameters κ_γ and λ_γ are related to the lowest order terms in a multipole expansion of photon interactions with the W :

electric charge

$$Q_W = e g_1^\gamma$$

magnetic dipole moment

$$\mu_W = \frac{e}{2m_W}\left(g_1^\gamma + \kappa_\gamma + \lambda_\gamma\right)$$

electric quadrupole moment

$$q_W = -\frac{e}{m_W}\left(\kappa_\gamma - \lambda_\gamma\right)$$

Anomalous value of κ_γ and / or λ_γ —> anomalous W magnetic moment

Form Factors

- Interaction Lagrangians with constant anomalous couplings violate unitarity at high energies

- The coupling parameters must be modified to include form factors, e.g. $WW\gamma$:

$$\Delta\kappa(q^2) = \frac{\Delta\kappa^0}{(1 + q^2/\Lambda^2)^n}$$

where:

$\Delta\kappa^0$ = value of coupling parameter at $q^2 = 0$

$q^2 = \hat{s}$ = square of the invariant mass of the $W\gamma$ system

$n = 2$ for a dipole form factor

Λ = form factor scale
(a function of the scale of new physics)

- Weak boson pair production at Fermilab probes the trilinear gauge boson vertices over a large range of $\hat{s}$ values

Effect of anomalous couplings

$$p\bar{p} \rightarrow W\gamma$$

1) Increase in the cross section
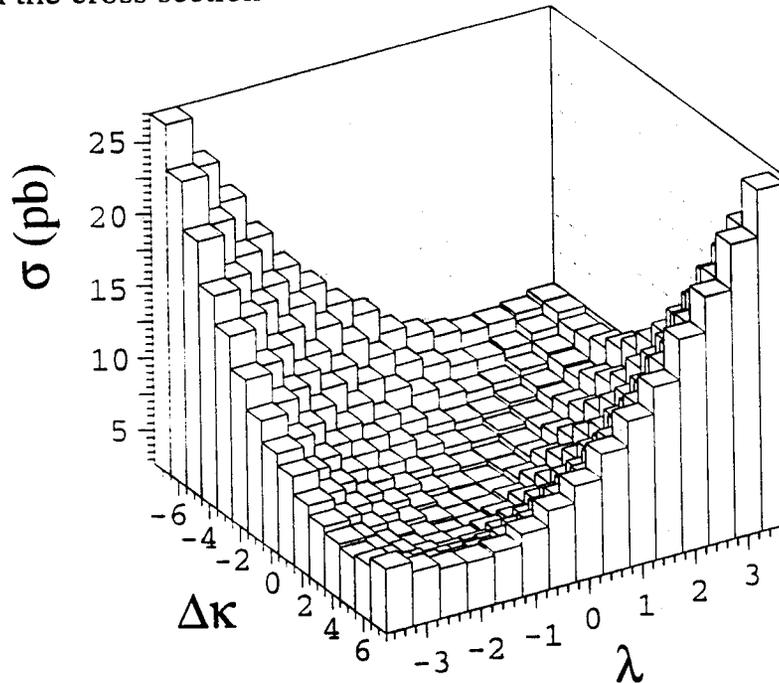
2) Enhancement of photons at high E_T – anomalous coupling effects are predominant at high $\sqrt{\hat{s}}$
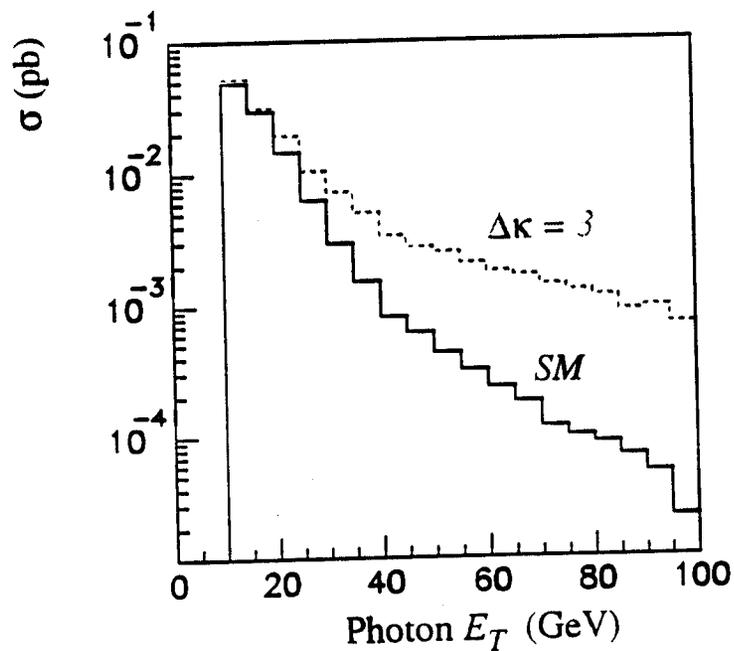
$W\gamma$ production cross section

- Photon kinematic selection:
$$E_T^\gamma > 10 \text{ GeV}$$
$$R_{l\gamma} > 0.7$$

	W(eν)γ	W($\mu\nu$)γ
N_{obs}	11	12
Backgrounds		
W + Jets	1.7 ± 0.9	1.3 ± 0.7
Zγ	0.11 ± 0.02	2.7 ± 0.8
W($\tau\nu$)γ	0.17 ± 0.02	0.4 ± 0.1
Total	2.0 ± 0.9	4.4 ± 1.1
N_{signal}	$9.0^{+4.2}_{-3.1} \pm 0.9$	$7.6^{+4.4}_{-3.2} \pm 1.1$
Acceptance	11 %	29 %
Efficiency	$(4.12 \pm 0.45)\%$	$(4.06 \pm 0.69)\%$

D$\emptyset$ data: $\quad \sigma(p\bar{p} \to W\gamma) = 138^{+51}_{-38} \text{ (stat)} \pm 21 \text{ (sys) } \textbf{pb}$

SM prediction: $\quad \sigma(p\bar{p} \to W\gamma) = 112 \pm 10 \text{ pb}$

Observed signal agrees with SM prediction within errors

$\to$ derive limits on $\Delta\kappa$ and λ to quantify experimental sensitivity to anomalous couplings

$W\gamma$ production – kinematic distributions
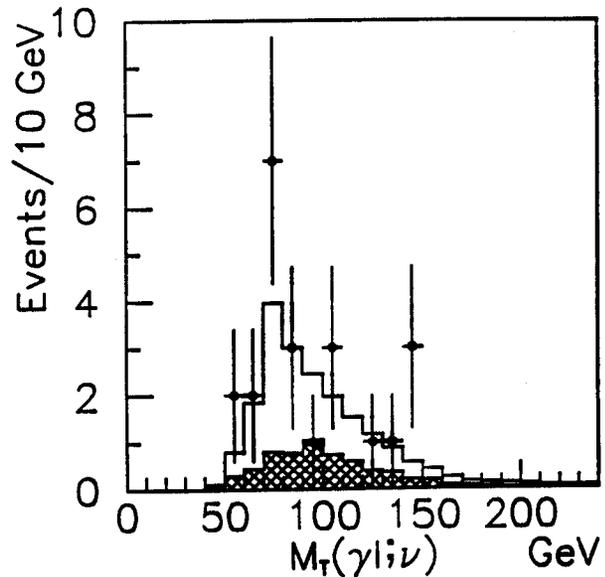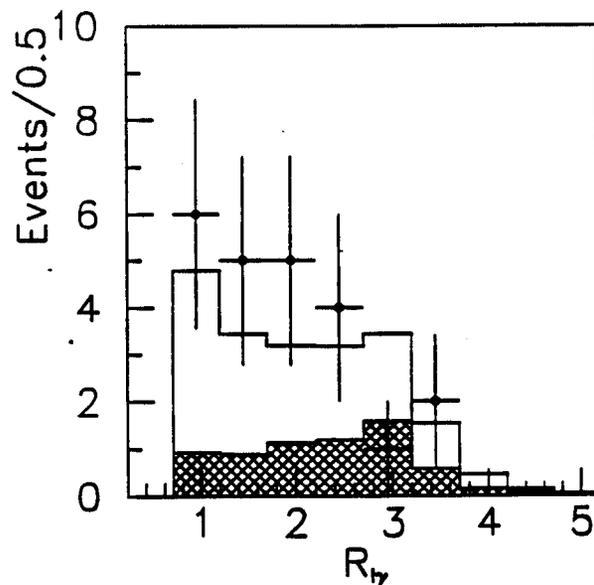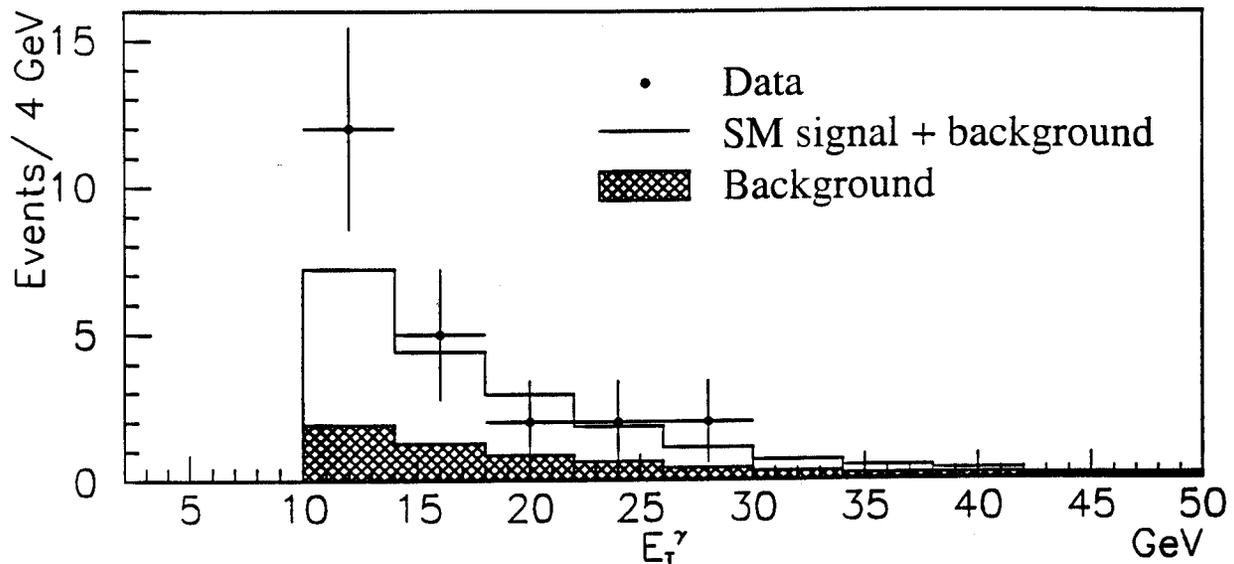
- $R_{l\gamma} = \sqrt{\Delta\eta_{l\gamma}^2 + \Delta\phi_{l\gamma}^2}$ = lepton–photon separation in R-space

- $M_T(\gamma l; \nu)$ = photon–lepton–neutrino cluster *transverse* mass

- Standard Model $W\gamma$ prediction is from the BAUR+BERGER event generator with DØ detector fast Monte Carlo
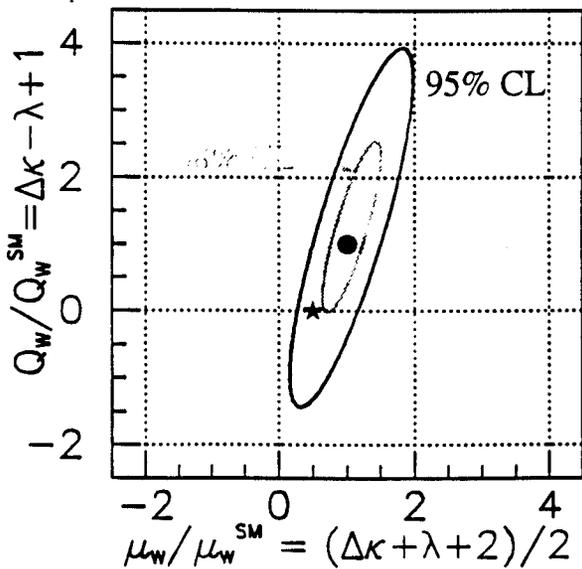
WWγ anomalous couplings – limits
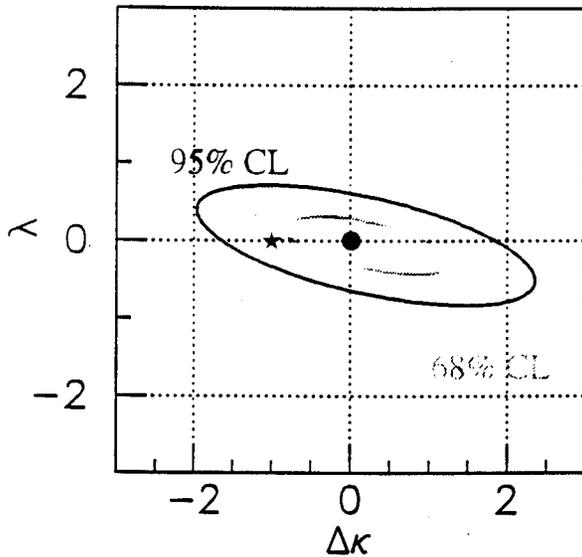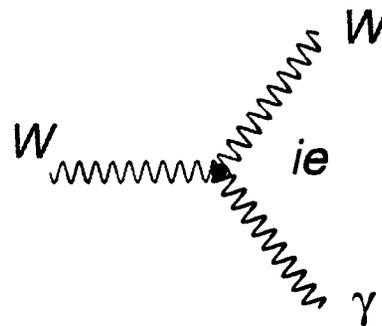

$\Lambda = 1.5 \text{ TeV}$

<u>95% CL Limits:</u>

$-1.6 < \Delta\kappa < 1.8$ for $\lambda = 0$

$-0.6 < \lambda < 0.6$ for $\Delta\kappa = 0$

$\bullet = \text{SM} \ (\kappa{=}1, \ \lambda{=}0)$

$\bigstar = U(1)_{EM}$ only coupling $(\kappa{=}0, \ \lambda{=}0)$:

$\rightarrow$ ruled out at 80% CL

*WW*γ anomalous coupling limits - comparison
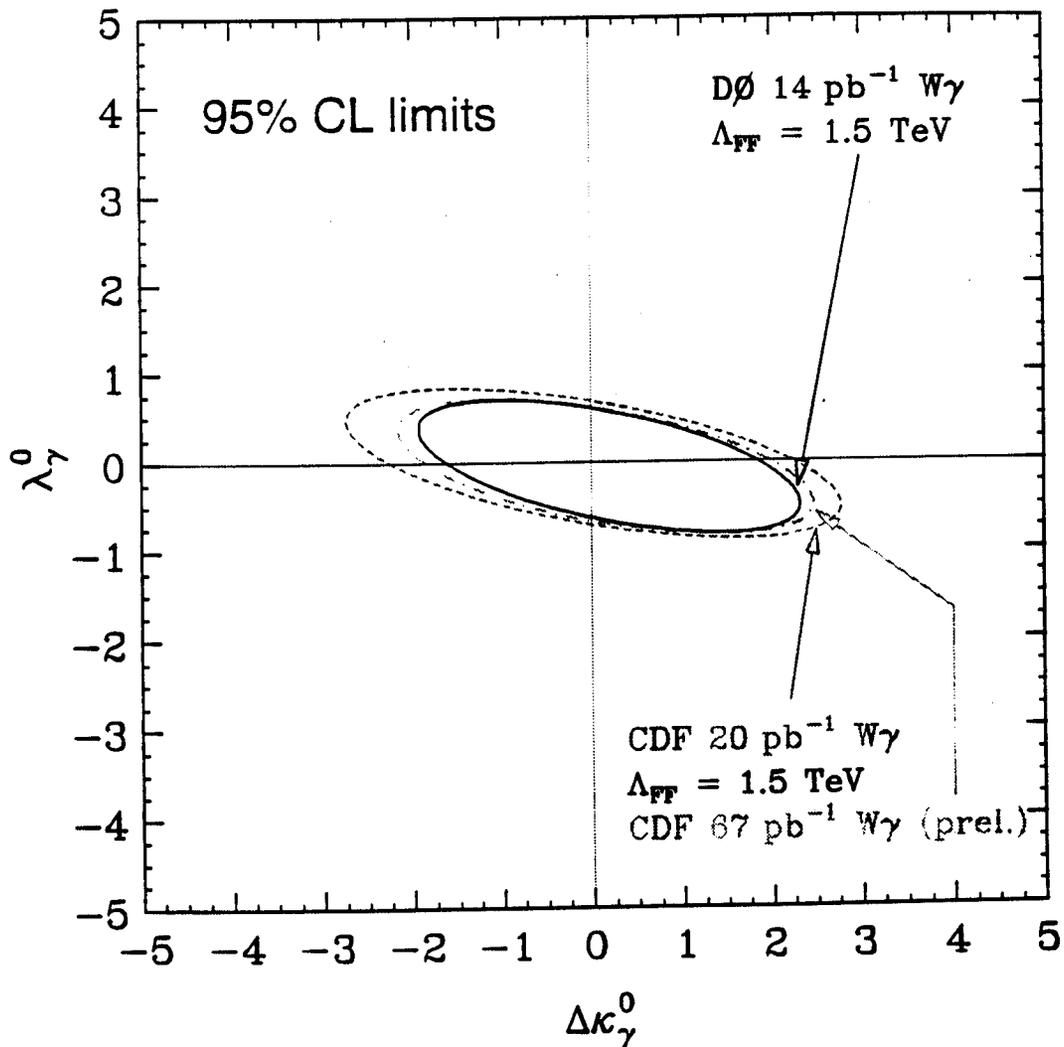
Run 1B Preliminary $W\gamma$ Results

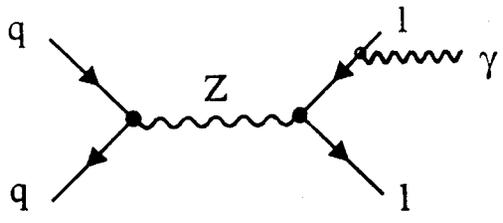- $W\gamma$ Photon E_T Distribution – electron channel only
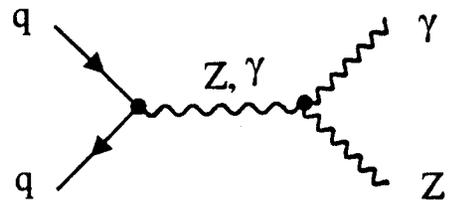

DØ Preliminary

$\int L\,dt = 55.2\ \text{pb}^{-1}$

- DØ Data (36 events)
— SM signal + background
(shaded histogram is
background only)

$\text{Nsignal} = 24.4\,{}^{+7.1}_{-6.0}\ \text{events}$

Number of Events / 10 GeV

Photon E_T (GeV)

<u>Zγ production</u>

A) u-channel

$q \longrightarrow$ ～～～ γ

$q \longleftarrow$ ～～～ Z

B) t-channel

$q \longrightarrow$ ～～～ Z

$q \longleftarrow$ ～～～ γ
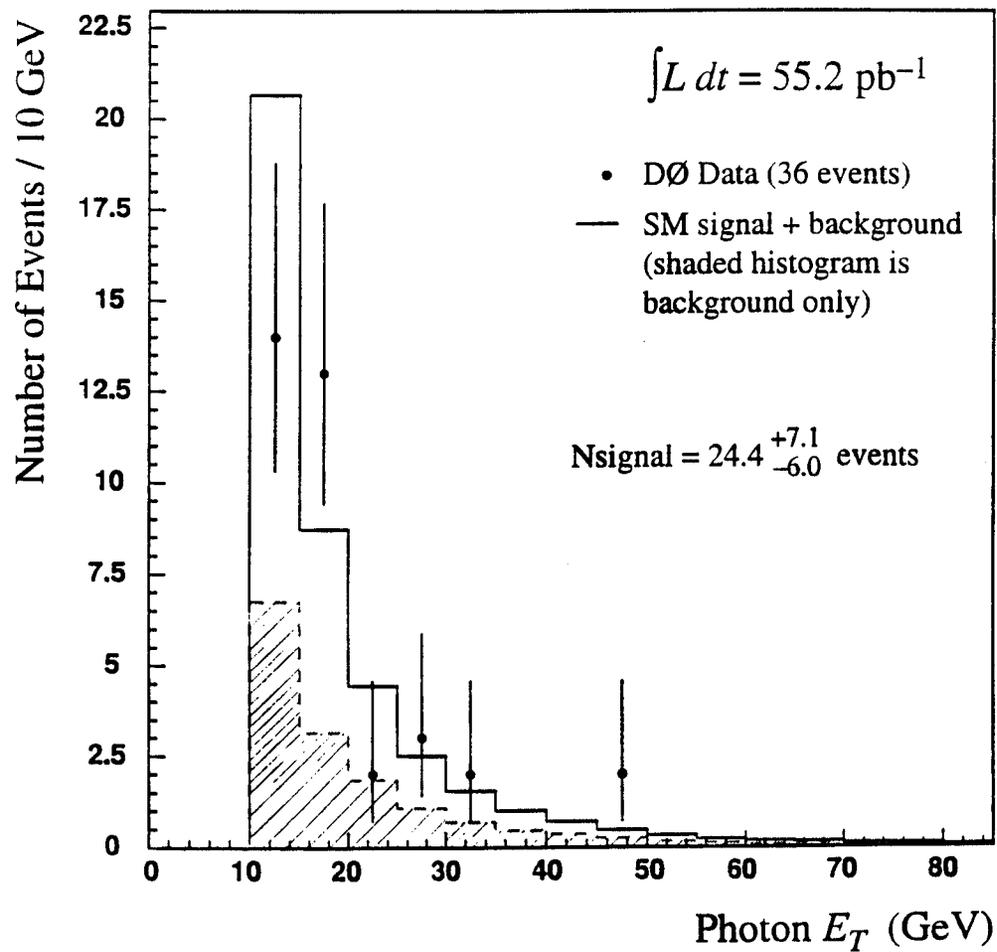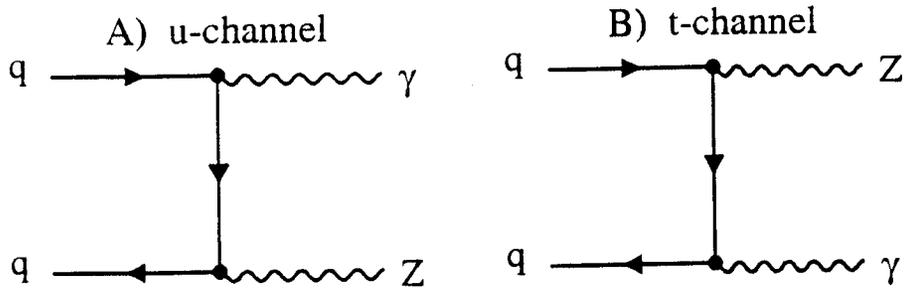
C) Inner Bremsstrahlung

q ＼ ↘

Z

q ↙ ∕

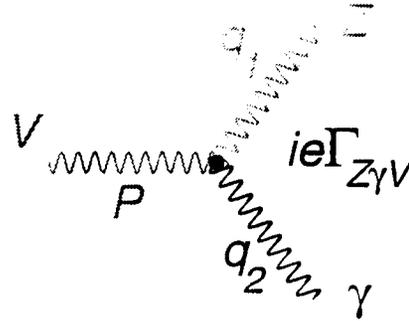l ～～～ γ

l

D) s-channel

q ↘

Z, γ

q ↗

γ

Z

The ZZγ and Zγγ vertices

Assume electromagnetic gauge
invariance and invariance under
Lorentz, C and P transformations

$V = \gamma, Z$

Parameterize $Z\gamma V$ in terms of the vertex Feynman rule:

$$\Gamma_{Z\gamma V}^{\alpha\beta\mu}(q_1, q_2, P) = \frac{P^2 - m_V^2}{m_Z^2}\left[h_3^V \varepsilon^{\mu\alpha\beta\rho} q_{2\rho} + \frac{h_4^V}{m_Z^2} P^\alpha \varepsilon^{\mu\beta\rho\sigma} P_\rho q_{2\sigma} \right]$$

where h_3^V, h_4^V are dimensionless couplings

In the SM at tree level (no coupling of γ to neutral Z),

$$h_3^V = 0, \quad h_4^V = 0$$

The vertex functions vanish at $P^2 = m_V^2$ because of:

> Gauge invariance   for $V = \gamma$
> Bose symmetry   for $V = Z$

$Z\gamma$ production

- Photon required with $E_T^\gamma > 10\,\text{GeV}$ and $R_{l\gamma} > 0.7$

	Z(ee)γ	Z($\mu\mu$)γ
N_{obs}	4	2
Backgrounds		
QCD	0.43 ± 0.06	0.02 ± 0.01
Z($\tau\tau$)γ	0.004 ± 0.002	0.03 ± 0.01
Total	0.43 ± 0.06	0.05 ± 0.01
N_{signal}	$3.57\,^{+3.15}_{-1.91} \pm 0.06$	$1.95\,^{+2.62}_{-1.29} \pm 0.01$
Acceptance	53 %	20 %
Efficiency	0.17 ± 0.02	0.06 ± 0.01
SM prediction	$2.8 \pm 0.3 \pm 0.2$	$2.3 \pm 0.4 \pm 0.1$

$Z\gamma$ production – photon E_T spectrum
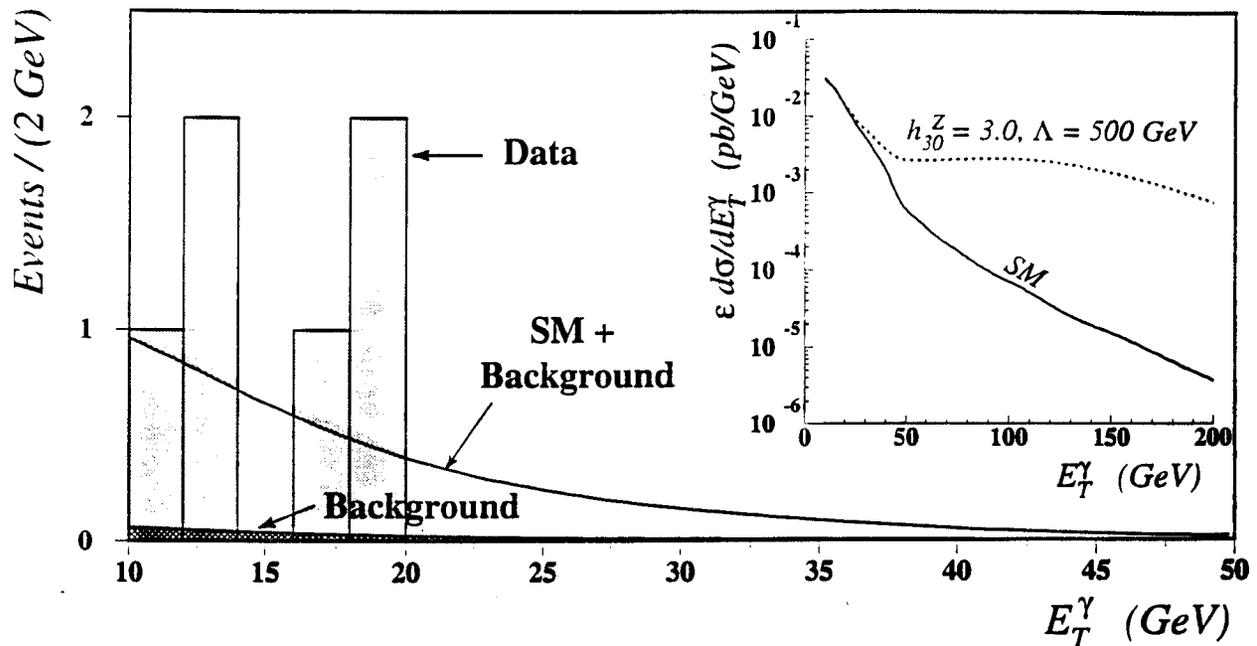
- Standard Model $W\gamma$ prediction is from BAUR+BERGER event generator with DØ detector fast Monte Carlo

- Inset shows the photon E_T spectra for SM and anomalous $ZZ\gamma$ coupling
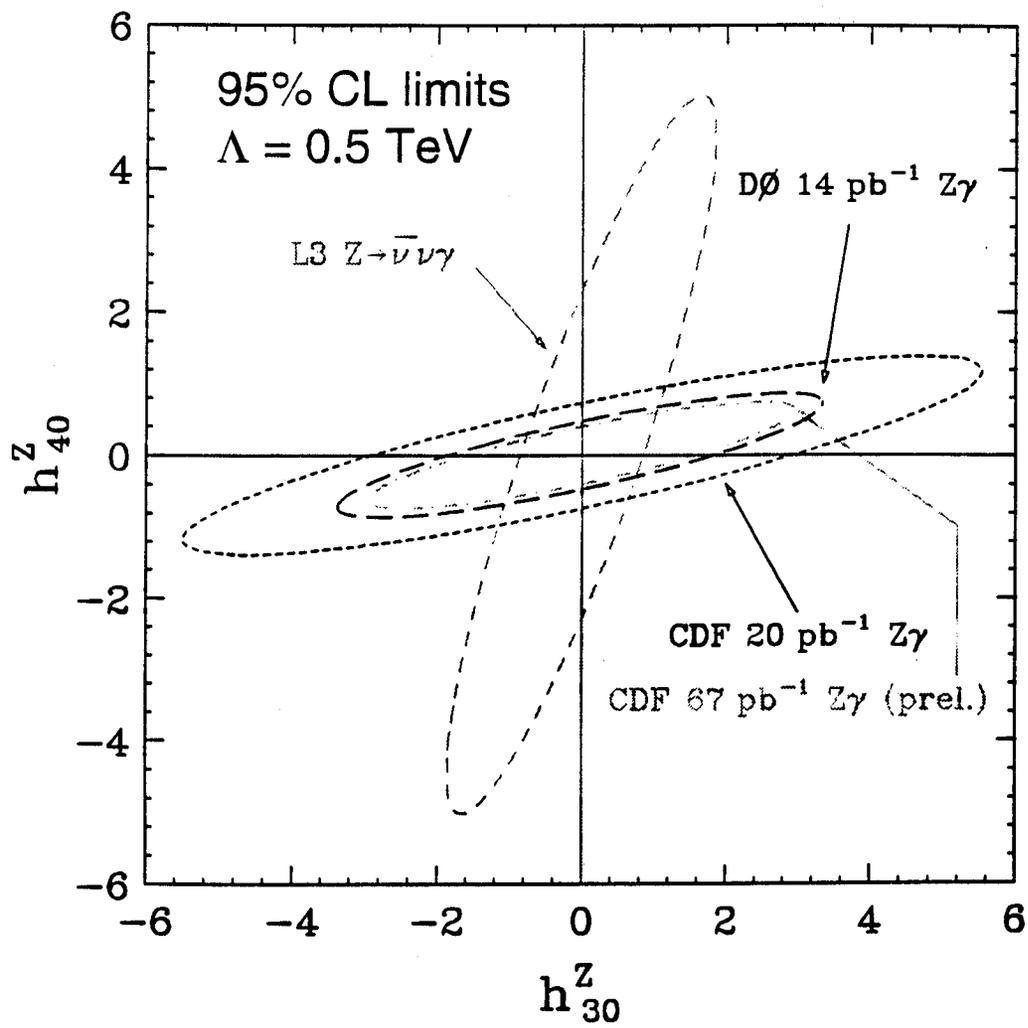
$ZZ\gamma$ and $Z\gamma\gamma$ anomalous couplings – limits
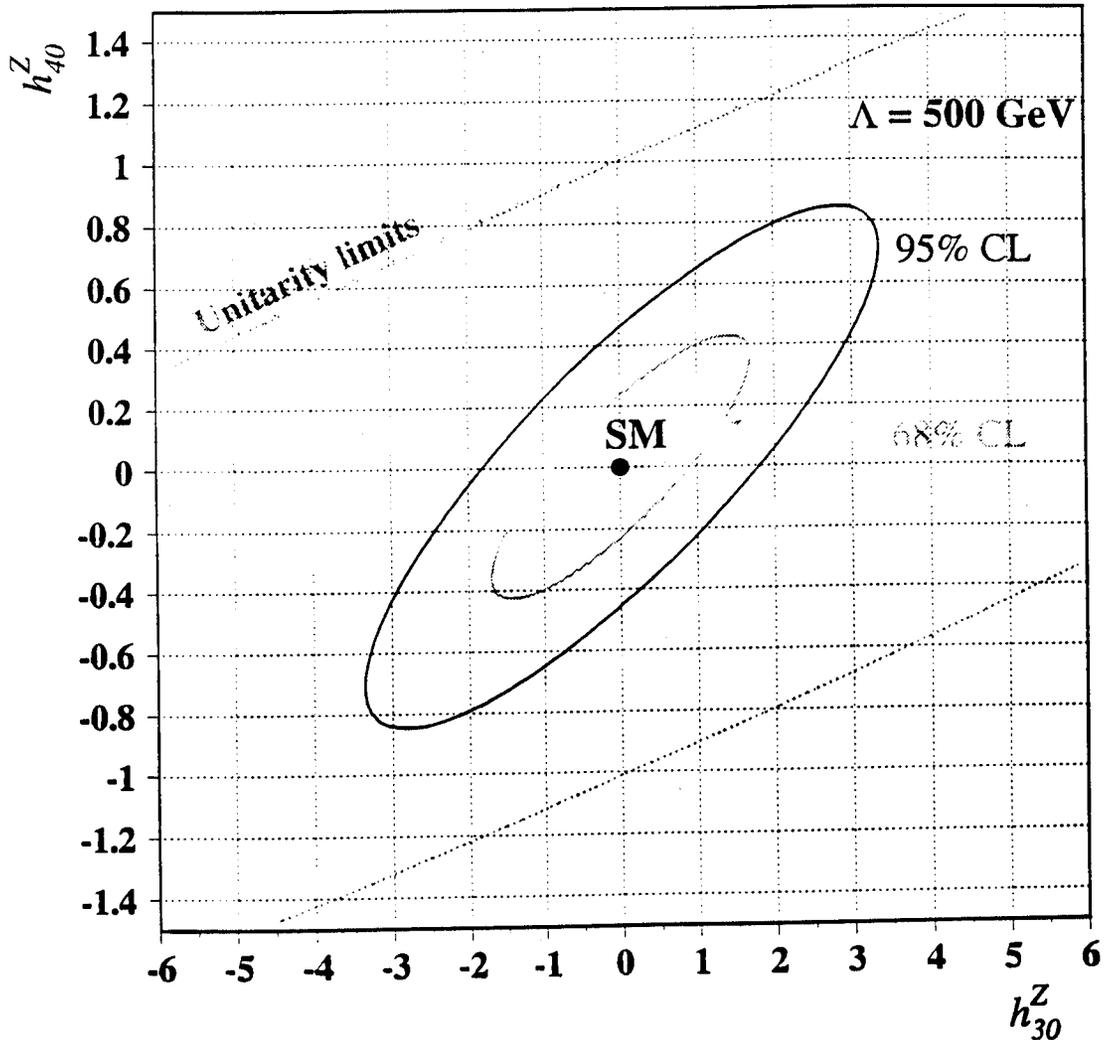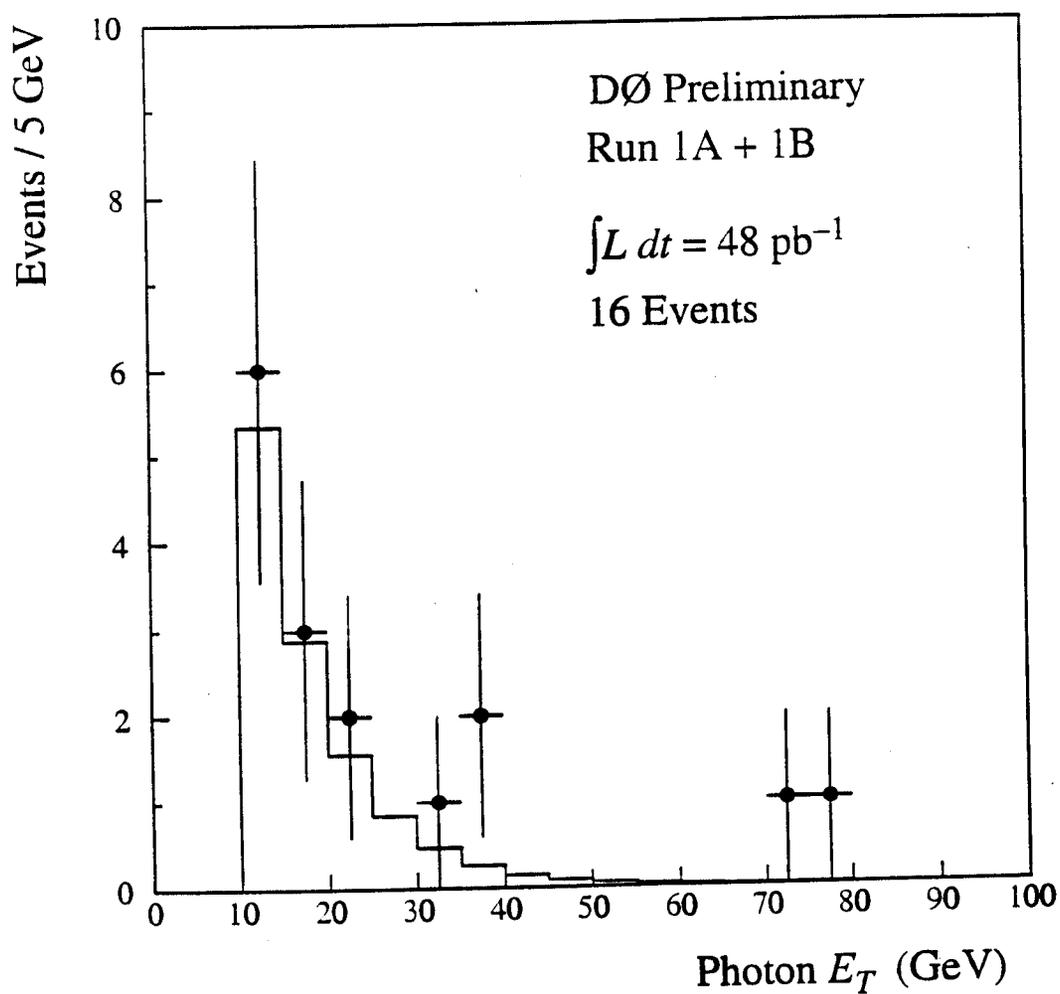

95% CL limits (for $\Lambda = 500$ GeV):

$$-1.8 < h_{30}^Z < 1.8 \qquad \text{for } h_{40}^Z = 0$$
$$-0.5 < h_{40}^Z < 0.5 \qquad \text{for } h_{30}^Z = 0$$
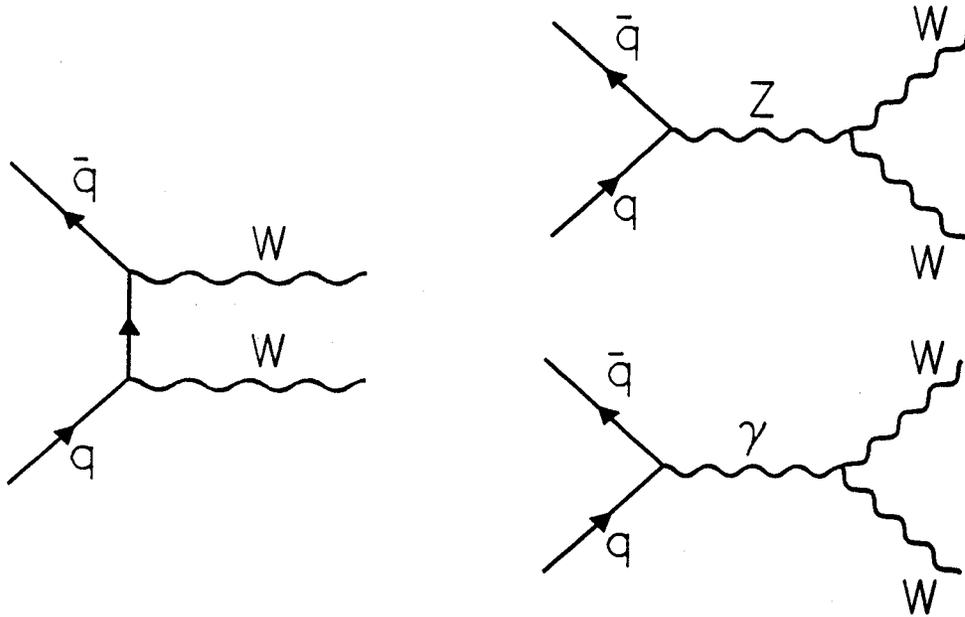
$ZZ\gamma$ anomalous coupling limits – comparison

Run 1B Preliminary $Z\gamma$ Results

- $Z\gamma$ Photon E_T Distribution – electron channel only

WW, WZ production

e.g $p\bar{p} \to W^+W^-$:

- *WW, WZ* $\to l\nu\, q\bar{q}$ "lepton + jets" decay mode

Signature: – high p_T electron, missing E_T, plus two jets

Backgrounds: – QCD multijet (jet fakes an electron)
    – W + $\geq$2jet production

- *WW* $\to l\nu\, l\nu$ "dilepton" decay mode
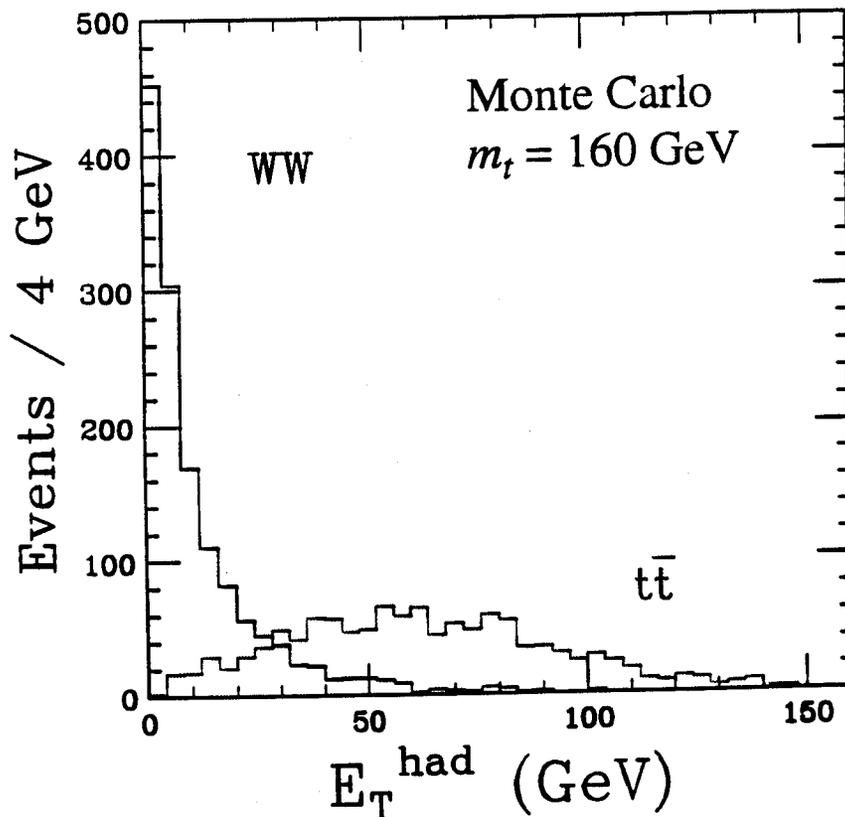
Signature: – two high p_T leptons, missing E_T

Backgrounds: – QCD, $W\gamma$, $Z \to ll$, $t\bar{t}$
    – much smaller than lepton + jets channel

$WW \rightarrow l\nu\, l\nu$ event selection

- Search in $e\mu$, ee, $\mu\mu$ channels

- Two high p_T leptons with missing $E_T > 20$ GeV

- To reject $t\bar{t}$ background, we use the vector sum of the E_T from hadrons:

$$\vec{E}_T^{had} = -(\vec{E}_T^{l1} + \vec{E}_T^{l2} + \not{E}_T)$$

- Require $E_T^{had} < 40$ GeV:
    - reduces $t\bar{t}$ background by a factor of 4 ($m_{top} = 160$ GeV)
    - effeciency for SM WW signal $= 95\%$

$WW \rightarrow l\nu\, l\nu$ candidates

- One event passes all the cuts (*ee* channel)

  SM prediction for *WW* signal = 0.47 ±0.07 events
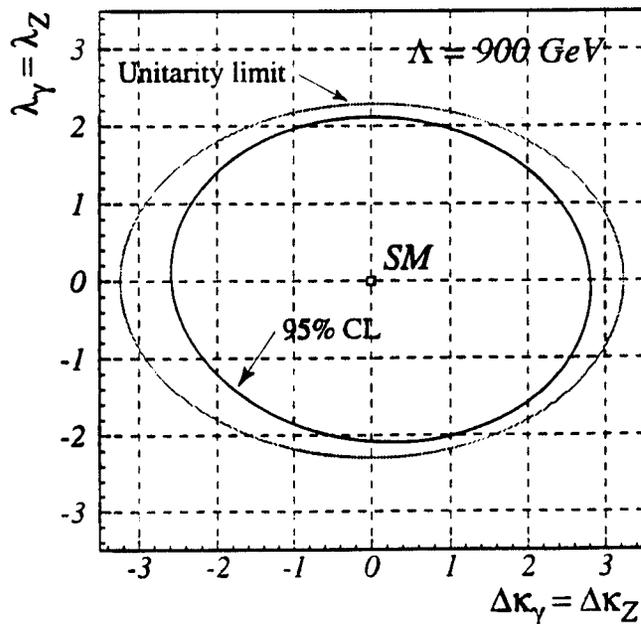
  Total estimated background = 0.56 ± 0.13 events

- The upper limit on the cross section for $p\bar{p} \rightarrow W^+W^-$ derived from this measurement is

$$\sigma\left(p\bar{p} \rightarrow W^+W^-\right) < 87 \text{ pb} \qquad 95\% \text{ CL}$$

  SM prediction = 9.5 pb
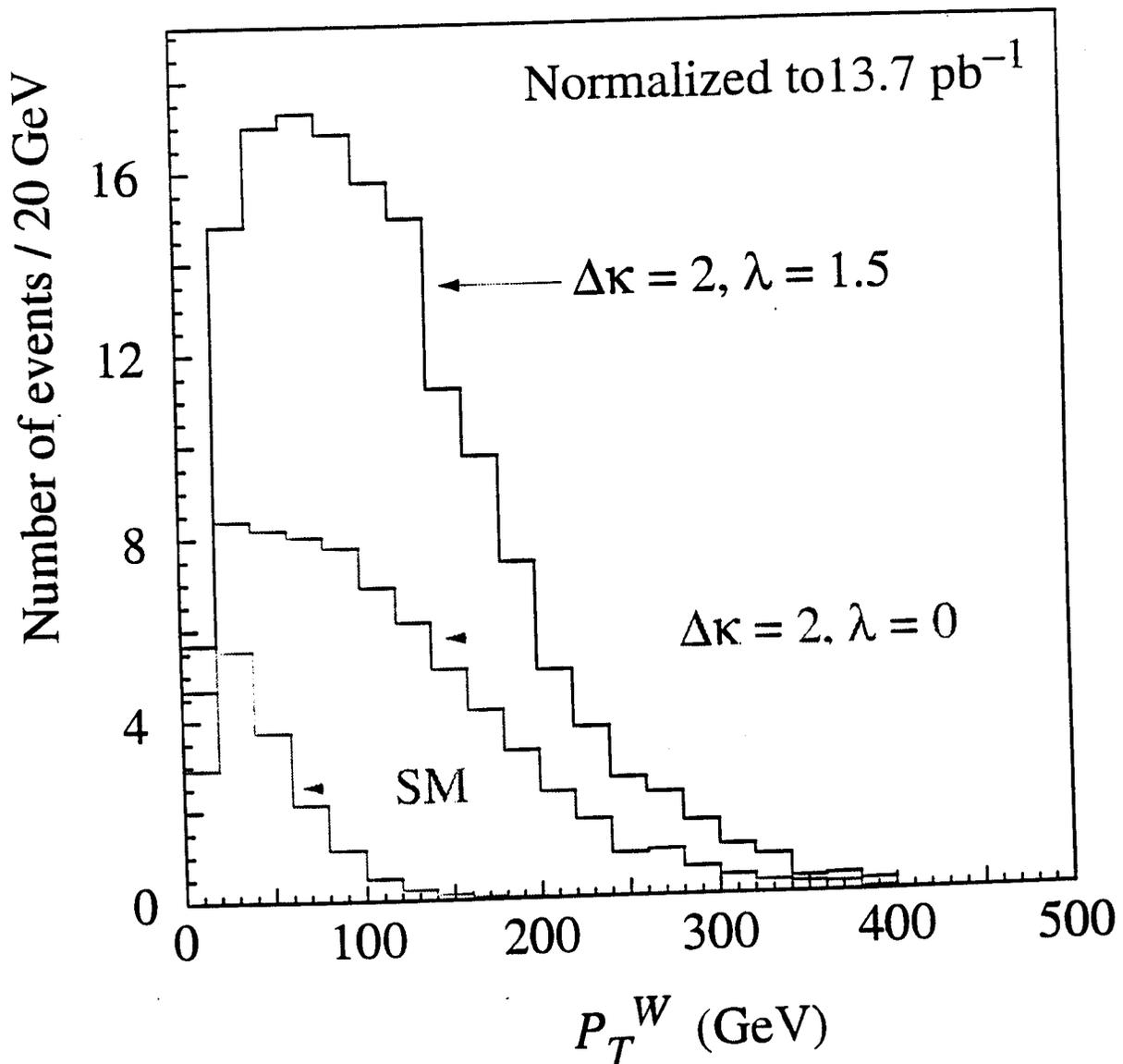
- The 95% CL limits on the coupling parameters are

$$-2.6 < \Delta\kappa < 2.8 \quad (\lambda = 0)$$
$$-2.1 < \lambda < 2.1 \quad (\Delta\kappa = 0)$$

  For $\Lambda = 900$ GeV at 95% CL
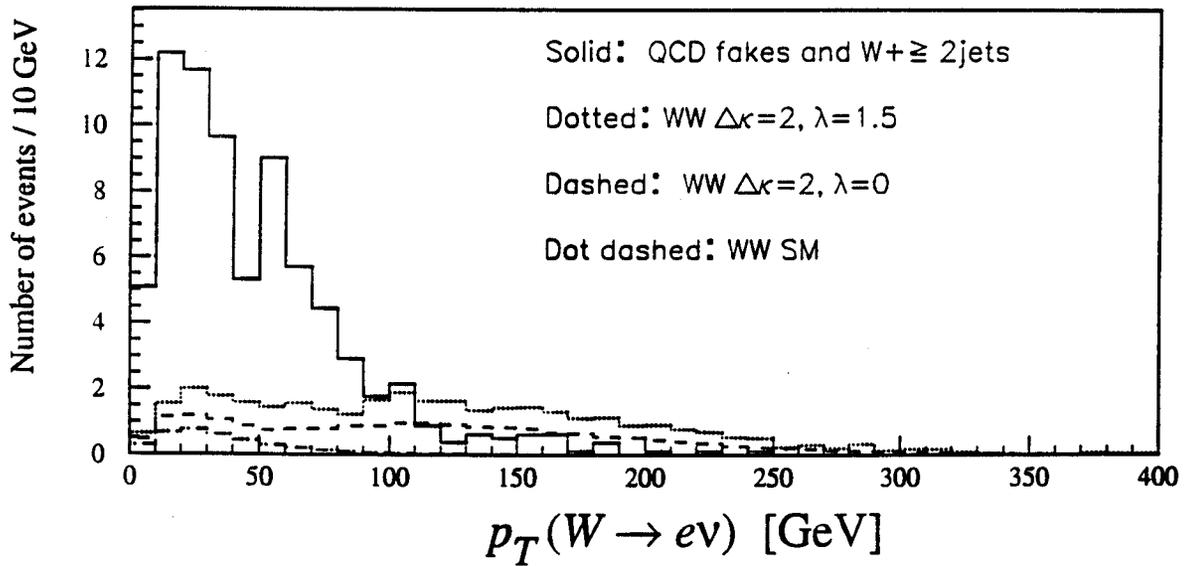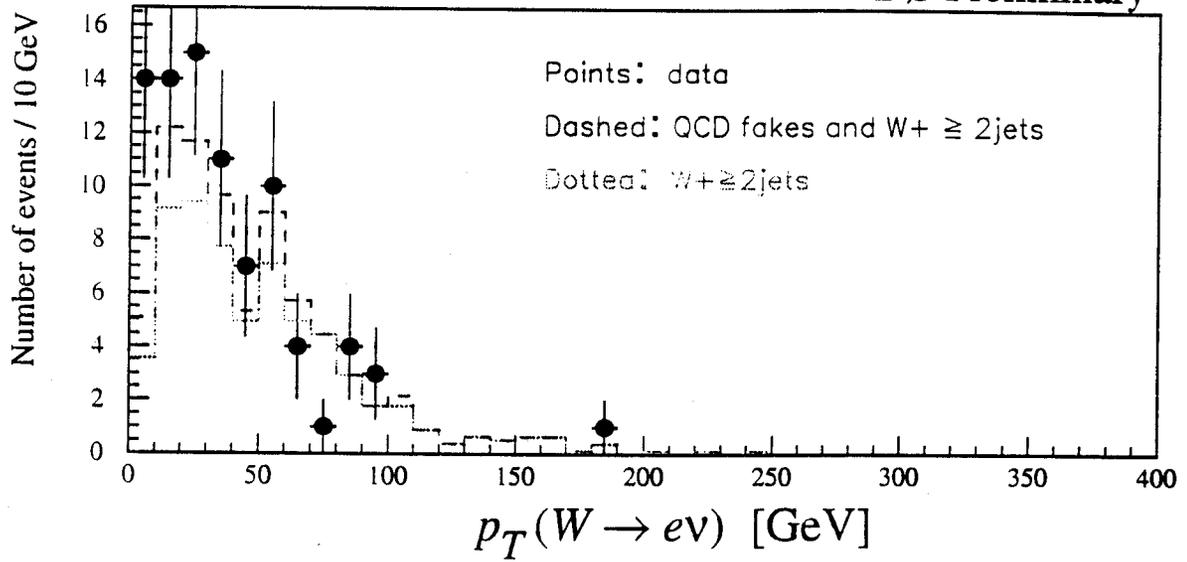
$WW, WZ \rightarrow l\nu \, jj$

- The $WW, WZ \rightarrow l\nu \, q\bar{q}$ channel is background dominated

- However, at high $p_T(W \rightarrow e\nu)$
  - backgrounds are small
  - anomalous $WW\gamma / WWZ$ couplings enhance cross section

$\rightarrow$ sensitive test of anomalous couplings

p_T^W spectrum

Points: data

Dashed: QCD fakes and W+ ≧ 2jets

Dotted: W+≧2jets

$p_T(W \to e\nu)$ [GeV]

Solid: QCD fakes and W+ ≧ 2jets

Dotted: WW $\Delta\kappa = 2$, $\lambda = 1.5$

Dashed: WW $\Delta\kappa = 2$, $\lambda = 0$
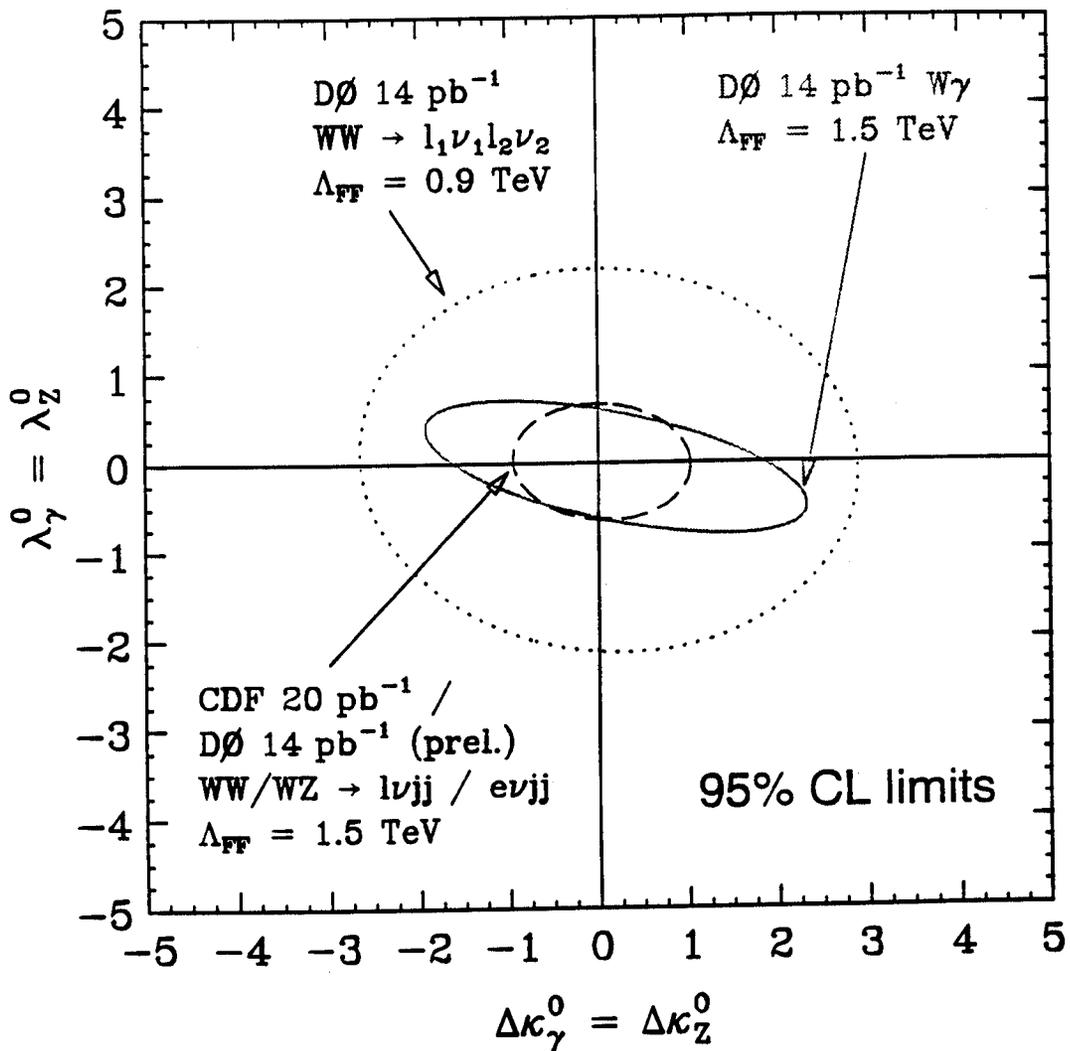
Dot dashed: WW SM

$p_T(W \to e\nu)$ [GeV]

- 95% CL limits obtained from binned likelihood fit, assuming $\Lambda = 1.5$ TeV and $\Delta\kappa_\gamma = \Delta\kappa_Z$, $\lambda_\gamma = \lambda_Z$:

$$-0.89 < \Delta\kappa < 1.07 \quad (\lambda = 0)$$

$$-0.66 < \lambda < 0.67 \quad (\Delta\kappa = 0)$$

WWV anomalous coupling limits – comparison

Tevatron limits on anomalous couplings

- Expected 95% CL limits for the Main Injector era:

Channel	Coupling	$1\ \text{fb}^{-1}$	$10\ \text{fb}^{-1}$
$W\gamma$	λ_γ^0	0.12	0.06
	$\Delta\kappa_\gamma^0$	0.4	0.2
$Z\gamma$	$h_{30}^{Z,\gamma}$	.04	.025
($\Lambda = 1.5$ TeV)	$h_{40}^{Z,\gamma}$	0.0025	0.0015
WW, WZ	λ_γ^0	0.2	0.15
($\Lambda = 2$ TeV)	$\Delta\kappa_\gamma^0$	0.4	0.25

i.e. couplings will be determined to approximately

$WWV \sim O(0.1)$
$Z\gamma V \sim O(10^{-2}\text{–}10^{-3})$

where $V = \gamma, Z$

- Observation of the radiation zero in $p\bar{p} \rightarrow W\gamma$

Summary and Conclusions

- DØ has measured the cross section times branching ratio for $W \rightarrow l\nu$ and $Z \rightarrow ll$ and used this to obtain the inclusive width of the W:

$$\Gamma(W) = 2.044 \pm 0.091 \text{ (expt.)} \pm 0.017 \text{ (theory) GeV}$$

- The W mass analysis is almost complete and we expect to have a final result soon

    - the energy scale uncertainty has been reduced to approximately 170 MeV

- Diboson production is in agreement with the SM predictions, within the experimental sensitivity . We set 95% CL limits on anomalous trilinear vector boson couplings of:

$W\gamma \, (\Lambda = 1.5 \text{ TeV})$
$$-1.6 < \Delta\kappa < 1.8 \quad \text{for } \lambda = 0$$
$$-0.6 < \lambda < 0.6 \quad \text{for } \Delta\kappa = 0$$

$Z\gamma \, (\Lambda = 500 \text{ GeV})$
$$-1.8 < h_{30}^{Z} < 1.8 \quad \text{for } h_{40}^{Z} = 0$$
$$-0.5 < h_{40}^{Z} < 0.5 \quad \text{for } h_{30}^{Z} = 0$$

$WW \, (\Lambda = 1.5 \text{ TeV})$
$$-0.89 < \Delta\kappa < 1.07 \quad (\lambda = 0)$$
$$-0.66 < \lambda < 0.67 \quad (\Delta\kappa = 0)$$